REPORT DOCUMENTATION PAGE

1. REPORT NUMBER	2. GOVT ACCESSION NO.	3. RECIPIENT'S CATALOG NUMBER
AFIT/CI/NR 86-136T		

4. TITLE (and Subtitle)	5. TYPE OF REPORT & PERIOD COVERED
Complex Principal Component Analysis of Sea Level Pressure Over Eastern North America and the Western Atlantic Ocean: A Search for Preferred Disturbance Activity Areas	THESIS/DISSERTATION
	6. PERFORMING ORG. REPORT NUMBER

7. AUTHOR(s)	8. CONTRACT OR GRANT NUMBER(s)
Frank Lively Estis	

9. PERFORMING ORGANIZATION NAME AND ADDRESS	10. PROGRAM ELEMENT, PROJECT, TASK AREA & WORK UNIT NUMBERS
AFIT STUDENT AT: North Carolina State University	

11. CONTROLLING OFFICE NAME AND ADDRESS	12. REPORT DATE
	1986
	13. NUMBER OF PAGES
	75

14. MONITORING AGENCY NAME & ADDRESS(if different from Controlling Office)	15. SECURITY CLASS. (of this report)
	UNCLASS
	15a. DECLASSIFICATION DOWNGRADING SCHEDULE

16. DISTRIBUTION STATEMENT (of this Report)

APPROVED FOR PUBLIC RELEASE; DISTRIBUTION UNLIMITED

DTIC
ELECTE
SEP 17 1986

B

17. DISTRIBUTION STATEMENT (of the abstract entered in Block 20, if different from Report)

18 SUPPLEMENTARY NOTES	
APPROVED FOR PUBLIC RELEASE: IAW AFR 190-1	LYNN E. WOLAVER Dean for Research and Professional Development AFIT/NR

19. KEY WORDS (Continue on reverse side if necessary and identify by block number)

20. ABSTRACT (Continue on reverse side if necessary and identify by block number)

ATTACHED ...

AD-A171 972

DTIC FILE COPY

ABSTRACT

The purpose of this study was to indentify preferred areas of synoptic

scale disturbance activity through the use of the objective analysis

technique called complex principal component analysis. The analysis

technique was applied to a sea level pressure data set consisting of

twice daily observations (00 and 12 GMT) during the months of January,

February, and March, for the years 1973-1976 and 1979-1982. The months

of January through March were chosen to encompass the time frame of the

Genesis of Atlantic Lows Experiment 1986. The geographical area studied

extended approximately from 30-120 degrees west and from 25-60 degrees

north.

The complex principal component analysis technique allows the

detection of propagating features in the pressure data set. The original

data set is augmented with its own Hilbert transform, which is nearly

equivalent in the time domain to the quadrature spectrum in the

frequency domain.

The variance in the pressure field is felt to be a direct

reflection of disturbance activity. Furthermore, when the data are

filtered to a "synoptic scale" frequency window, the variance in the

pressure field corresponds closely with cyclone and anticyclone storm

tracks over a time period of two to ten days.

The results of the analysis produced four components that could be

given a preliminary interpretation from a physical sense. The components

(patterns) resembled areas of activity as discovered in previous studies

using other subjective analysis techniques.

COMPLEX PRINCIPAL COMPONENT ANALYSIS OF SEA LEVEL

PRESSURE OVER EASTERN NORTH AMERICA AND THE

WESTERN ATLANTIC OCEAN: A SEARCH FOR

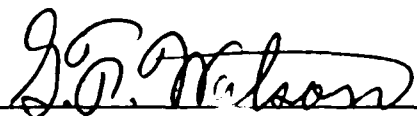PREFERRED DISTURBANCE ACTIVITY AREAS

by

FRANK L. ESTIS

A thesis submitted to the Graduate Faculty of
North Carolina State University
in partial fulfillment of the
requirements for the Degree of
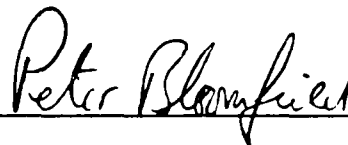Master of Science

DEPARTMENT OF MARINE, EARTH AND ATMOSPHERIC SCIENCES
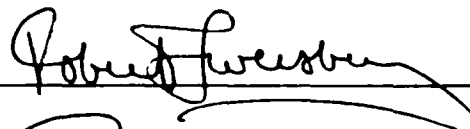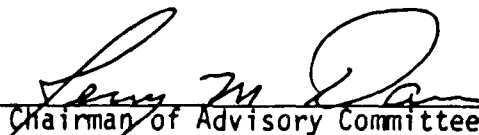

Raleigh

1986

APPROVED BY:

Chairman of Advisory Committee

BIOGRAPHY

Frank L. Estis was born in Richmond, Virginia, on February 8,
1954. He was reared in the same community and graduated from Henrico
High School, Henrico County, Virginia, in 1972.

He entered the Virginia Military Institute in August of 1972 ard
received a Bachelor of Science degree with a major in Chemistry in May
of 1976. He was commissioned as a second lieutenant in the United
States Air Force that same month.

The author has been assigned to the following locations since
entering the Air Force:

Texas A&M University	AUG 1976 - AUG 1977
Seymour Johnson AFB, Goldsboro, NC	AUG 1977 - JUL 1980
Finthen AAF, Mainz-Finthen, West Germany	JUL 1980 - SEPT 1982
Bitburg AB, Bitburg, West Germany	SEPT 1982 - AUG 1984

In August 1984 the author entered the Graduate School at North
Carolina State University and began studies toward a Master of Science
degree in Meteorology.

The author is married to the former Ann Scott Capehart of
Richmond, Virginia.

ACKNOWLEDGEMENTS

TABLE OF CONTENTS

TABLE OF CONTENTS (continued)

LIST OF TABLES

Page

LIST OF FIGURES

LIST OF FIGURES (continued)

1. INTRODUCTION

Considerable time and effort have been devoted to the study of synoptic cyclones and anticyclones and their preferred areas of genesis and movement. Synoptic scale cyclones (lows) and anticyclones (highs) have wavelengths of 1000 to 2500 km, as seen in the lower troposphere. They are recognized on synoptic surface weather charts as migratory low- and high-pressure systems, respectively. This keen interest in synoptic scale disturbances is understandable since the daily weather we experience is closely related to the cyclones and anticyclones that form, move across, and dissipate over the earth's surface. These disturbances are features of the general circulation and, as such, have preferred areas of activity as controlled by the general circulation.

As indicated by Barber et al. (1984) there have been many studies of the spatial distribution of cyclone activity (anticyclone studies are fewer in number), and a few studies that examined the temporal variations in synoptic scale disturbance activity. Most of these studies are based on counts of individual disturbances on daily weather maps or on published disturbance track maps. These subjective counting techniques have some inherent problems associated with them, including changing methods of map analysis and interpretation, changing data density over time, and unequal grid areas with changing latitude.

To overcome these problems an objectively determined meteorological variable is needed which is accurately measured and whose variance is related to the synoptic scale disturbance activity. Barber et al. (1984) chose the station pressure as the variable

required. It is accurately measured, and studies by Klein (1951a, 1951b), Blackman et al. (1977), Hartmann (1974), and Barber et al. (1984) strongly suggest that there is a spatial correspondence between synoptic scale disturbances and the variance in station or sea level pressure, especially if the pressure data are filtered to look at an appropriate "synoptic scale" frequency window with a period of approximately 2-10 days.

Barber et al. (1984) applied spectral analysis techniques to a limited data set (3 data stations) to test the usefulness of the station pressure as an indicator of disturbance activity and found further support for the relationship between synoptic scale disturbances and the variance in the station pressure field. The recently documented analysis technique called complex principal component analysis (Barnett, 1983; Horel, 1984) appears to be a promising technique to apply to a geographically larger data set of pressure values to look for relationships between the variance in the pressure field and synoptic scale disturbance activity.

Complex principal component analysis (CPCA) in the time domain is designed to take a set of linearly interdependent variables, which are functions of space and time, and transform (rotate) the original configuration of observations to a new orientation having the same number of dimensions (variables) but where the new orientation consists of a set of mutually orthogonal (independent) dimensions. These new dimensions (components) are linear composites of the original variables and account for the variation in the original variables. The components accounting for the largest amounts of variance in the

original data can be used to study/interpret the physical processes taking place in the original data set. Since the components are orthogonal, they can be combined in various ways or studied separately. Sometimes a large percentage of the variation in the original variables can be accounted for by the first few largest components. This is the goal of CPCA--to reduce the number of dimensions needed to "explain" a data set using new dimensions that are linearly independent.

CPCA allows the efficient detection of propagating features in a geophysical data field that are derived from the interaction between traveling and standing waves of different spatial scales and temporal frequencies (Horel, 1984). CPCA should allow the separation of the preferred patterns (areas) of synoptic scale disturbances from the overall variance in the sea level pressure field since the individual disturbances are guided by the standing and traveling waves in the general circulation patterns.

The sea level pressure was chosen as the variable to use in this study versus the station pressure used by Barber et al. (1984). By using the sea level pressure the elevation of the observation stations is eliminated as a variable in the computations. Standard observational practice is to reduce the observed station surface pressure to a value that would exist at a point at sea level directly below the station, if the temperature at sea level is assumed to be the same as the temperature at the higher elevation station. The actual method used to reduce the pressure uses the preceding 12-hour mean temperature, not the instantaneous temperature at the time of the station pressure observation. This introduces some error into the

pressure observations, but not enough to outweigh the advantages of eliminating the elevation as a variable.

The objectives of this study are to 1) apply the objective analysis technique, CPCA, to a sea level pressure data set and try to detect the preferred areas and movement of synoptic scale disturbances; 2) document the areas and movement discovered and show their agreement or disagreement with previous study results; 3) and explain the limitations and problems encountered during this study effort and how they affected the results of this analysis.

2. PRELIMINARY DATA PROCESSING

The data used in this study are the final analyses of the sea level pressure field, for the Northern Hemisphere, as analyzed by the U.S. Navy using the objective analysis scheme called "Fields by Information Blending" (Holl and Mendenhall, 1971). The data set was obtained from the data archives of the National Center for Atmospheric Research (NCAR). There are two maps per day, at 00 and 12 GMT, for the time periods from 1 January to 31 March, for the years 1973 to 1976 and 1979 to 1982.

The NCAR data set contains sea level pressure values (hereafter referred to as SLP) interpolated to an octagonal grid system which is a square grid overlaid on an octagonal area of a polar stereographic projection of the earth's surface. The grid points are approximately 324 km apart, depending on the latitude (for further details, see Jenne, 1970, 1975). See figure 2a for the geographical area covered by the data set used in this study.

The time period of 1 January to 31 March was selected to encompass the time frame of the Genesis of Atlantic Lows Experiment (GALE) 1986. The preferred areas of synoptic disturbance activity and their movement during the winter months were of interest for GALE purposes. Of particular interest are the cyclones that develop off the Atlantic coast and intensify rapidly as they move northward. The data set years of 1973-1976 and 1979-1982 were selected based on the fact they had the least number of observational maps missing (approximately 1 percent), and no more than one map missing consecutively. This allowed the

replacement of missing maps with the values obtained from a linear
interpolation from neighboring values in time.

The mean SLP at each individual grid point, for January through
March for each year, was calculated and subtracted from the individual
SLP observations in the respective yearly time series. The time series
were adjusted slightly to compensate for leap years in 1976 and 1980.
The SLP deviations were then Fourier transformed and the Fourier
coefficients for periods greater than 10 days or less than 2 days were
set equal to zero. The inverse transform resulted in a band-passed
filtered time series with information only in the desired time interval
of synoptic scale events.

The period described above was based on previous work which showed
disturbances in this time interval "exhibited variance and covariance
patterns characterized by elongated maxima suggestive of storm tracks
and an association with baroclinic waves" (Blackmon et al., 1984a), and
that these disturbances contribute the most to the spectrum of the
variance when studying the time period from .25 to 18.75 days (Barber
et al., 1984). Other studies by Blackmon (1976), Blackmon and White
(1982), Blackmon et al. (1977, 1979, 1984a, 1984b), White (1980), and
Hartmann (1974) all suggest a spatial and temporal correspondence
between cyclones/ cyclone tracks, and variance of SLP and other
parameters at upper levels in the atmosphere (e.g., 850 mb temperature
deviations; 700, 500, 300 mb height deviations). Care must be
exercised as regions of high variance may also correspond to tracks of
anticyclones as well as cyclones (Klein, 1951b), and this was found to
be the case as discussed later.

3. BACKGROUND THEORY AND METHODS

The development, in the meteorological literature, of CPCA in the time domain can be traced back to Rasmusson et al. (1981), while CPCA in the frequency domain appeared first in Wallace and Dickinson (1972). In this section a brief summary of relevant theory will be presented along with the methods used in this study.

a. decomposition theory

The work of Rasmusson et al. (1981) was based on the Singular Value Decomposition (SVD) theorem. The theorem supports the relationship between an arbitrary real nxm ($n \leq m$) matrix $A = \{A_{ij}\}$ and a summation:

$$A_{ij} = \lambda_1 X_i^{(1)} Y_j^{(1)} + \lambda_2 X_i^{(2)} Y_j^{(2)} + \ldots + \lambda_n X_i^{(n)} Y_j^{(n)} , \qquad (1)$$

with $\lambda_1 \geq \lambda_2 \geq \ldots \lambda_n \geq 0$, where the λ's are referred to as singular values and the $\{X_i^{(\ell)}\}_{i=1,n}$ and $\{Y_j^{(\ell)}\}_{j=1,m}$ are known as the ℓth left and right singular vectors, respectively.

The theorem can be expressed in matrix form as

$$A_{nxm} = X_{nxr} \Delta_{rxr} Y'_{rxm} , \qquad (2)$$

where X and Y are each orthonormal sections and Δ is a diagonal matrix of ordered positive singular values. The prime denotes the transpose. The rank of A is given by r, the number of positive values. The columns of X and Y are the left and right singular vectors, respectively, of A. The left singular vectors (columns of X) are the eigenvectors of the product AA', and the right singular vectors (columns of Y) are the eigenvectors of the product A'A. Thus, the

eigenvectors are derived from A. Each of these product matrices has eigenvalues given by the respective singular value squared. That is, the matrix Δ_{rxr} is a diagonal matrix whose main diagonal entries are the square roots of the positive common eigenvalues of AA' and A'A (Green, 1978).

If the original matrix, A, which was n x m, had observations of a variable in time indexed by i = 1,2,...n, and grid point locations indexed by j = 1,2,...m, then the operation AA' would produce a n x n matrix which contains only information concerning the temporal characteristics of the original matrix A. The operation A'A produces a m x m matrix which contains only information concerning the spatial characteristics of the matrix A. The SVD technique thus allows the separation of information describing the data matrix under study. Additionally, since the Δ_{rxr} matrix contains singular values common to both the AA' and A'A matrix operation results, the most important terms from AA' and A'A can be selected to describe A based on the magnitude of the associated squared singular values.

The leading terms of the expansion, (1), constitute an efficient basis for describing a given data array. The terms can be ordered so that the terms with the largest λ's are first in the expansion since the terms are orthogonal and the vectors have unit length. It can be shown that this expansion is best in the least squares sense. The magnitude of λ directly establishes the importance of each term in the expansion--the leading terms accounting for the largest portion of the variance in the given array, and succeeding terms accounting for smaller and smaller portions of the variance.

The potential usefulness of this decomposition method is realized when it is applied to a data set containing features that are highly correlated on broad scales. A few leading terms of the decomposition (expansion) will usually contain the most meaningful information contained in the matrix, while the remaining terms contain signals considered noise. It should be easily seen that in calculating the eigenfunction of one product matrix Y (=A'A), the eigenfunction of the other product matrix X (=AA') follows from a simple matrix multiplication operation when using the SVD technique.

The SVD theorem outlined above can be altered to include complex matrices also. All matrix transpose operations, indicated by the prime notation, would become complex conjugate transpose operations. Additionally, the references to $Y_j^{(\ell)}$ in (1) would become the complex conjugate of $Y_j^{(\ell)}$.

While the decomposition of a real nonsymmetric matrix is usually referred to as SVD, the decomposition of a real symmetric cross products matrix (i.e., correlation matrix, covariance matrix, etc.) is often referred to as principal components analysis (PCA).

b. principal components theory

The SVD of a data matrix, A, can be found with A defined as

$$A = (A_{ij} - \overline{A}_j) , \tag{3}$$

where $i = 1, 2, \ldots n$ and $j = 1, 2, \ldots m$, and $\overline{A}_j$ is the mean of each column of A. Define also the covariance matrix, C, as

$$C = A'A / (m-1) . \tag{4}$$

The SVD of a symmetric cross product matrix (C in this case) takes the form

$$C = UDU' , \tag{5}$$

where U is an orthogonal matrix of eigenvectors and D is a diagonal matrix of C's eigenvalues. Thus it can be seen that the SVD of a symmetric product moment matrix provides (Green, 1978): 1) a matrix of eigenvalues D in the decomposition of C which is equal to $\Delta^2/(m-1)$, as would be obtained from the SVD of the matrix A; 2) a matrix of eigenvectors U in the decomposition of C which is exactly the same as Y in the SVD of A.

If the matrix product A'A has been constructed to contain spatial information only, then after computation of U (=Y) we can find Z such that

$$Z = AU = X\Delta , \tag{6}$$

where Z contains the temporal information originally contained in A. We will refer to the columns of U (eigenvectors) as the components (which show spatial variation) and to the columns of Z as the component scores (which show temporal variation).

The components can be viewed as sets of direction cosines that rotate the original data matrix to a new set of mutually orthogonal component axes. If the component's values are plotted at their respective grid points and contoured, the areas of low and high variability in the data field will be revealed. The values of the components are in relative units. The component scores, Z = AU, are

the projection of the original data observations onto the component
axes. The scores indicate how important an observation is in
interpreting a component. When the scores are plotted as a time
series, the plot will reveal at what time the observations had the
greatest variability. The units of the scores are the same as the
units on the original variables. The eigenvalues contained in the
matrix, D, indicate how much of the total variance of the original data
set is accounted for by each pair of components and component scores.
The units of the eigenvalues are the same as the units on the original
variables, but squared.

Many standard meteorological variables are interdependent in space
or time, or both--some related in ways so complex that physical cause
and effect links are not clear. PCA transforms a set of
intercorrelated variables into a new coordinate system in which the
axes are linear combinations of the original variables and are mutually
orthogonal (Hayden and Smith, 1982). The objectives of the PCA are to:
1) untangle complex patterns of intervariable association in
multivariate data; 2) isolate characteristic, recurrent, and
independent patterns of covariance among the variables into a new set
of independent variables; and 3) reduce the dimensionality of the set
of multivariate data and still retain its most important features.

PCA can be considered a closed system model in that all the
variance in the original variables is being investigated (Johnston,
1978). The analysis technique does not depend on any predetermined
form, but rather depends upon the interrelationships within the data
being analyzed. The form of the component's patterns is determined
empirically from the fundamental data. The variance of a scalar (or

vector) field can be represented by comparatively few independent
coefficients of the eigenvectors when plotted spatially, and the
associated patterns may in some cases be given a physical
interpretation.

If the eigenvectors are derived from a covariance matrix, their
spatial form depends directly on the coherence of the departures from
normal over the area of analysis. The eigenvector patterns will
reflect the real spatial distribution of variance over the study area.
If the covariance matrix is based on SLP data, the resulting
eigenvector patterns should represent synoptic patterns. The pattern
represented by the eigenvector (component) associated with the largest
eigenvalue can be thought of as representing the mean pattern of
variability in the data field (Johnston, 1978).

PCA has a major limitation in that it only resolves instantaneous
temporal covariance; thus anomalies that move in space and time cannot
be fully identified (Michaelsen, 1982). It can only portray variations
in time as either in phase or 180° out of phase. So it cannot be used
to represent features with variable phase relationships, such as
traveling waves.

c. frequency domain CPCA

Wallace and Dickinson (1972) developed what has been called CPCA
in the frequency domain (hereafter referred to as FDPCA). They were
trying to develop a technique to avoid problems inherent in
cross-spectral analysis of data sets where there are more than one type
of wave structure present in the same frequency band, i.e., there is no

way to determine how many significant wave structures are present or their relative contribution to the variance spectra.

Wallace and Dickinson's new technique involved computing the cross-spectrum matrix of the data set, where the diagonal elements o, the matrix are the power spectral estimates obtained by crossing each time series with itself, and the off-diagonal elements are complex, the real part being the co-spectrum and the imaginary part the quadrature spectrum. The original data set was first band-passed filtered to eliminate all components outside the frequency band of interest. The vector time series are expressed as a linear combination of the eigenvectors of the cross-spectrum matrix. The eigenvectors are applied to an augmented time series involving the original time series and its time derivative.

Wallace and Dickinson (1972) showed that a time series $u_j(t)$ has a spectral representation (analogous to Fourier representation),

$$u_j(t) = \text{Re} \int_{\omega=0}^{\infty} \exp(i\omega t) \, dA_j(\omega) \, , \tag{7}$$

where $dA_j(\omega)$ is a random increment function for an interval $d\omega$. Formation of the u_j correlation matrix with lag τ gives:

$$U_{jl}(\tau) = \langle u_j(t) \; u_l(t+\tau) \rangle$$

$$= \frac{1}{2} \, \text{Re} \int_{\omega=0}^{\infty} \exp(-i\omega\tau) \langle dA_j(\omega) dA_l^*(\omega) \rangle \, , \tag{8}$$

where * denotes complex conjugate. If $\tau = 0$, $U_{jl}(\tau)$ reduces to a covariance matrix. The covariance matrix formed by the $dA_j(\omega)$ gives

the contribution to $U_{j1}(\tau)$ by the cross spectrum $\phi_{j1}(\omega)$ in an infinitesimal frequency interval $d\omega$:

$$\phi_{j1}(\omega) \, d\omega = \frac{1}{2} < dA_j(\omega) \, dA_1^*(\omega) > . \tag{9}$$

If a filtered series $u_j{}^f(t)$ is defined

$$u_j{}^f(t) = Re[\exp(i\omega t) \, dA_j(\omega)] \, d\omega , \tag{10}$$

then the filtered correlation matrix $U_{j1}{}^f(\tau)$ is

$$U_{j1}{}^f(\tau) = Re[\exp(-i\omega\tau)\phi_{j1}(\omega)] . \tag{11}$$

If PCA is applied to the filtered time series, it would involve finding the eigenstructure of the symmetric matrix $U_{j1}{}^f(o)$, or equivalently $Re[\phi_{j1}(\omega)]$. But this would lose the phase information contained in the quadrature components of the cross spectra, which is the very information needed to detect and separate traveling waves in the data set.

Since ϕ_{j1} is Hermitian, it has a complete set of orthonormal eigenvectors and real eigenvalues, but the eigenvectors are now complex. Wallace and Dickinson (1972) then showed how to find this eigenstructure which was then applied to an augmented time series, $v_j(t)$, involving the original time series and its time derivative, so that the component scores, Z, took the form

$$z_i(t) = Re \sum_j e_{ij} v_j(t) , \tag{12}$$

where e_{ij} is the appropriate eigenvector.

d. time domain CPCA

While FDPCA would allow the study of propagating phenomena in a data set, it can be cumbersome in certain situations. If the power of a component is spread over a wide frequency band, then separate maps for each spectral estimate must be studied in order to document the propagating phenomenon (Horel, 1984). Rasmusson et al. (1981), Barnett (1983), and Horel (1984) have all developed and documented the idea of CPCA in the time domain (hereafter referred to simply as CPCA) which can be easier to use than FDPCA. CPCA is essentially FDPCA averaged over all frequency bands. CPCA is an efficient detector of propagating features, especially when the variance is spread over a number of frequencies (Horel, 1984).

Description of propagating features (waves) in a data set requires both co-spectrum and quadrature information. In the FDPCA as described by Wallace and Dickinson (1972), this information was contained in the cross-spectrum matrix $(\dot{\cdot}_{j1})$, and extracted and contained in the eigenstructure of the matrix so propagating disturbances could be detected. In the time domain this information is not so readily available. This information can be obtained through the use of the Hilbert transform. The following theory describing the use of the Hilbert transform is based on the work of Barnett (1983).

A scalar field $u(x_j,t)$, where j is a spatial position index and t is time, has a Fourier representation of the form:

$$u_j(t) = a_j(\cdot) \cos \cdot t + b_j(\cdot) \sin \cdot t , \qquad (13)$$

where the Fourier coefficients (a,b) at positive frequencies are

defined in the usual manner. The variable, u, is then described by a complex representation, i.e.,

$$U_j(t) = \sum_\omega c_j(\omega)\, e^{-i\omega t} , \tag{14}$$

where $c_j(\omega) = a_j(\omega) + ib_j(\omega)$ and $i = \sqrt{-1}$. Expanding (14) and collecting terms yields

$$U_j(t) = \sum_\omega \{[a_j(\omega) \cos \omega t + b_j(\omega) \sin \omega t]$$

$$+ i[b_j(\omega) \cos \omega t - a_j(\omega) \sin \omega t]\}$$

$$= u_j(t) + i\, \hat{u}_j(t) . \tag{15}$$

The real part of (15) is just $u_j(t)$ from (13). The imaginary part of (15), $\hat{u}_j(t)$, represents $u_j(t)$ phase shifted $\pi/2$ in time and is called the quadrature function or Hilbert transform of $u_j(t)$.

Wallace and Dickinson (1972) had quadrature information available in the frequency domain from (11) unless they used zero lag, in which case there would only have been the same information that would be available from a real valued covariance matrix in the time domain. This zero lag covariance matrix problem is eliminated in the time domain by going into the frequency domain through the Fourier transform, (13), and then summing over frequencies the quadrature information contained there, (15), and capturing it as the imaginary part of a complex number when returning to the time domain via the inverse Fourier transformation. This û is roughly equivalent in the time domain to the quadrature spectrum in the frequency domain. This is because the $\pi/2$ phase shift of incremental Fourier component is

equivalent to providing optimum lag information on that component.
Thus, in a sense, the information on relative phase among the elemental
sinusoids has been summed together. It is also obvious that the
frequency bandwidth of interest (time period) can be limited by
applying a band-pass filter to the original data set, or by limiting
the frequency range of summation in (15).

The covariance matrix of $U_j(t)$ is

$$C_{jk} = < U_j^*(t) \ U_k(t) >_t , \tag{16}$$

where * denotes complex conjugation and $< \ ... \ >_t$ indicates a time
averaging process. Usually C_{jk} would be a zero lag covariance matrix
containing no phase relationship information. But in this case, C_{jk}
has been constructed from U(t) which has the phase information built
into it. Since C is the complex "zero lag" covariance matrix, it can
be shown from standard spectral analysis theory that

$$C_{jk} = \int_0^{\omega_n} \phi_{jk}(\omega) \ d\omega , \tag{17}$$

where ϕ_{jk} is the complex cross-spectrum and ω_n the Nyquist frequency.
So C_{jk} represents the cross spectral matrix averaged over a specific
frequency band.

C is *Hermitian by construction and has real eigenvalues* (λ_n) *and*
complex eigenvectors, $B_n(x)$, where x represents spatial dependence. U
has a representation which optimally accounts for the variance in
u(x,t) in the time period (frequency band) under study, i.e.,

$$U(x,t) = \sum_n A_n(t) \ B_n^*(x) , \tag{18}$$

where the complex time-dependent component scores are given by

$$A_n(t) = \sum_x U(x,t)\, B_n(x) .$$ (19)

Four measures that define possible moving features in u(x,t) can be defined. To help clarify the interpretation of these measures a simple example is carried along with each definition with u(x,t) = a sin(kx-ω_0t), i.e., a wave of constant amplitude and frequency propagating in the positive x direction. The measures are:

1) spatial phase function $\theta_n(x)$: this function shows the relative phase of fluctuations among the various spatial locations where u is defined. This measure varies continuously between 0 and 2π, and an arbitrary reference value must be selected for it. The function is defined as

$$\theta_n(x) = \arctan\,[\text{Im } B_n(x)/\text{Re } B_n(x)] .$$ (20)

For the example being used, the data field is composed of a single sinusoid with wavelength L moving along the x axis. There is only one component, and $\theta_1(x)$ will go through one complete cycle (2π) over a distance L measured in the x direction, i.e., $\theta_1(x) = kx = 2\pi x/L$. If the data set covered a spatial area of 8000 km in width in the x direction and the sinusoid had a wavelength of 4000 km, then the spatial phase function should progress for 0 to 360 degrees twice in the x direction. [Note that the VAX/VMS version 4 FORTRAN intrinsic function ATAN2D was used in the computation of the spatial and temporal phase function, and it has a range from -180 < result < 180 degrees.]

2) spatial amplitude function $S_n(x)$: a measure of the spatial distribution of variability associated with each component. The distribution of S gives a measure of the spatial homogeneity, by component, in the magnitude of the u-field.

$$S_n(x) = [B_n(x) B_n^*(x)]^{1/2} . \tag{21}$$

For the constant amplitude sinusoid example being used, S_1 equals a constant since the amplitude, a, is independent of x. The spatial plot of this function would show equal values of amplitude at all grid points.

3) temporal phase function $\phi_n(t)$: this measure describes the temporal variation of phase associated with $u(x,t)$, by component, and is defined as

$$\phi_n(t) = \arctan [\text{Im } A_n(t)/\text{Re } A_n(t)] . \tag{22}$$

The example sinusoid of fixed frequency and wavenumber will have $\phi_1(t) = \omega_0 t = \text{constant} \times t$. The phase will progress from 0 to 360° over equal time intervals.

4) temporal amplitude function $R_n(t)$: this measure of temporal variability in the magnitude of the modal structure of the u-field is defined as

$$R_n(t) = [A_n(t)A_n^*(t)]^{1/2} . \tag{23}$$

The example sinusoid has $R_1 = \text{constant}$ over time, i.e., the plot will be a straight line at a constant value.

The functions described in (20) to (23) above constitute a general description of possible moving features in u. Extraction of the components of the covariance matrix, C_{jk}, allows the study of the largest spatially coherent "signals" present in the data set. This

analysis technique allows the eas, investigation, in time and space, of the dynamic behavior of energetic events that might well be obscured in a normal spectral analysis approach (Barnett, 1983).

e. methods

The data set used in this study, as described earlier, consisted of the deviations of SLP from the individual grid point yearly means. These eight sets of deviations (180 observations in each time series at 280 grid points) were filtered to concentrate on a certain frequency band (time period) (described in section 2), and to augment the deviations with their Hilbert transform. The filter used was developed from the theory presented by Cizek (1970). The filter had the form:

$$H_k = \begin{cases} 0 \ , & K = 1,2,\ldots,135 \quad \text{and} \quad 173, 174, \ldots, 180 \\ +2 \ , & K = 136, 137, \ldots, 172 \ . \end{cases} \tag{24}$$

This filter was applied to the data set while in the frequency domain, (13), and produced the desired band-passed filtered data set (2-10 days) with its Hilbert transform via the inverse Fourier transform.

These eight yearly filtered data sets were used to form eight Hermitian covariance matrices which were then summed. The summed matrix was then diagonalized to find the eigenvectors and eigenvalues using the IMSL (International Mathematical and Statistical Library) subroutine EIGCH. The eigenvectors (components) were ordered by their associated eigenvalues, and then the component scores were computed. From the components and component scores, the four functions as described in section 3.d.1)-4) were computed for the four components

having the *four largest eigenvalues.* *These four components were*
selected for study after preliminary analysis of the spatial phase and
amplitude function plots revealed they could be interpreted as synoptic
events. Components 5 through 280 were not interpretable, and
therefore, for this study's purposes, considered noise.

The spatial amplitude and phase plots were analyzed using a
computer graphics program which put the spatial phase plot "in motion"
while overlaid on the spatial amplitude plot. A color scheme was used
where over a 360-degree phase angle change the color representing the
phase would change from red, to green, to blue, and then start over
again. This changing of colors, as the computer scans the phase angle
data and assigns a color based on the phase angle value, appears to put
the plot "in motion." This greatly enhances the ability to see the
motion of the fluctuations in the data, as represented by the spatial
phase angle changes. The values of the spatial amplitude plot were
used to control the intensity of the colors, so the phase changes could
be detected more easily in the areas of greater variability. Results
are reported in section 5.

4. INTERPRETATION LIMITATIONS

Before considering the results of the interpretation of the component patterns from the CPCA, it is important to understand some of the limitations that affect the interpretation. Some of the limitations can be overcome through rotation of the initially computed components, and these techniques have been demonstrated by Richman (1981) and Horel (1981) for PCA. Horel (1984) outlined the method to be used for CPCA, but it appears to have a shortcoming, which is also discussed in this section.

One of the limitations of any type of principal component analysis is that the component shapes depend on the geometry of the domain, since the covariance between two variables can be considered the kernel of an integral equation eigenvalue problem (e.g., see North et al., 1982). The integral extends over the finite domain of interest. So if the shape or size of the domain is changed, the component patterns should be expected to change.

When computing the components of the data set, the first component is positioned in hyperspace to account for the largest amount of variance over all the data points, with each succeeding component orthogonal to it and to the other components to follow. Each succeeding component accounts for the maximum residual variance remaining in the input data matrix. Problems frequently arise when the first component locates between two or more distinct clusters of interrelated variables. In this study these variables would be stations located nearest to synoptic cyclone or anticyclone anomaly systems (Kutzbach, 1967; Richman, 1981). Another rotation would be

needed to accurately locate the data clusters so the component maps can be interpreted as an individual synoptic map type (e.g., see Richman, 1981, for comparison of rotation techniques). Rotated patterns generally contain somewhat stronger anomalies covering smaller portions cf the domain of interest. This "regionality" of fluctuations is very desirable.

Due to the orthogonality constraint placed upon the components of the data matrix, they may take on predictable geometric relationships to one another. If the first component is of one sign over the domain (applies to PCA), the second component pattern may be bipolar and have a zero line passing through the highest value of the first component pattern, and so on for the other components (Horel, 1981). In the case of CPCA, all component variability patterns are positively valued, but low variability areas on one map may match the high variability areas on another.

Linear transformation (rotation) of the components is performed to overcome the problems mentioned above. A variety of procedures exist to accomplish the rotation, e.g., varimax, quartimax, promax, oblimax (Richman, 1981; Horel, 1981; Green, 1978), all of which should identify regional relationships from the initial component solution. In the case of conventional PCA, using real data sets, these rotation procedures present no problems.

In the PCA of a data set the components can be thought of as orthogonal lines that bisect the axes' origin. These lines have both a positive and negative valued segment. Either segment can be used as a measure of the variance accounted for by the component of interest.

The negative or positive coefficient is associated with the phase (direction of the line) of the component. The phase is only known to within an additive constant (either 0 or π), so the sign of the component is ambiguous.

In the CPCA approach the phase angle is known only to within an additive constant that ranges from 0 to 2π. This indeterminancy is a problem when linearly transforming (rotating) the complex components. As outlined by Horel (1984), using the varimax rotation technique, an element, e_{jn}, of the nth complex eigenvector of a complex correlation matrix, can be written as

$$e_{jn} = <U_j(t)^{\star}A_n(t)>_t = S_{jn}e^{i\theta_{jn}} \quad , \tag{25}$$

where e_{jn} is the complex correlation between the jth time series and the nth component, S_{jn} is the magnitude of the correlation, and θ_{jn} is the phase. An estimate $U_j'(t)$ of the observation matrix $U_j(t)$ can be reconstructed with the first N' complex components where N' < N, where N is the total number of complex components as

$$U_j'(t) = \sum_{n=1}^{N'} e_{jn}^{\star}A_n(t) \ . \tag{26}$$

The estimate $U_j'(t)$ can be described in terms of the transformed (rotated) solution as

$$U_j'(t) = \sum_{n=1}^{N'} g_{jm}^* F_m(t) \ , \tag{27}$$

where $F_m(t)$ is an element of the nth rotated complex correlation (RC$\dot{}$C) and g_{jm} is the complex correlation between the nth RCPC and the jth observation of $U_j'(t)$.

In PCA the total amount of variance explained by the first component is maximized

$$\lambda_1 = \sum_{j=1}^{J} e_{j1}^2 \ , \tag{28}$$

where e_{j1} is the (real) correlation between the jth time series and the first component. Likewise, CPCA maximized

$$\lambda_1 = \sum_{j=1}^{J} e_{j1}^* e_{j1} \ , \tag{29}$$

where e_{j1} is a complex correlation and e_{j1}^* is its complex conjugate. PCA and CPCA maximize the sum of the squares of the amplitudes of the correlation coefficients. The varimax rotation technique maximizes a second moment statistic (the variance), rather than a first moment statistic (the sum) of the squared correlation coefficient. This causes strong regional relationships in large data sets to be emphasized.

In order to achieve this variance maximization, the complex loadings g_{jm} are expressed in terms of the complex eigenvectors e_{jn}:

$$g_{jm} = \sum_{n=1}^{N'} t_{mn} e_{jn} ,$$ (30)

where the coefficient t_{mn} of the transformation (rotation) matrix T are real. The maximization of the variance is dependent on e_{jn}, which can be seen from (25), to depend on a phase angle known only to within an arbitrary additive constant. Unlike the PCA case where the phase angles are 0 or π, the CPCA has as possible solutions a whole set of vectors ranging from 0 to 2π, each as valid a solution as the other. Thus, it appears that a maximization of the variance for a whole set of e_{jn}'s (as a function of the phase angle) is needed and then determination of which one gives the "best" maximization of the variance. If two or more maximizations are nearly equal, then a selection of the best solution must be based on the physical interpretation of the solutions--which one gives the best physical representation of the data.

Therefore, the initial components found in this study were not rotated, but rather interpreted as they were. More work needs to be done in the area of rotation of complex components, so that the rotation will not be dependent on an arbitrary phase angle. Then the rotation procedure will be of a manageable nature, where it doesn't require the computation of a large number of variance maximizations.

To see if the four unrotated components studied were suffering from the limitations outlined above, a squared coherence check was performed between the components. The components are orthogonal at zero lag, but may have coherence at any frequency. The squared

coherence check reveals if there is coherence present. Table 1 shows the squared coherence, by frequency, for the pairs of components. A value of .122 equals the 95 percent point of the null distribution of squared coherence. The 99 percent point equals .181.

The spectra of the four components, figure 1, show the important periods to be 6.4 to 5.6 and 5.0 to 4.5 days for component one; 9.0 to 8.2 days for component two; 9.0 to 6.4 days for component three; and 9.0 and 6.9 days for component four. An examination of table 1 shows that all pairs of components, except 2 and 4, have significant coherence at the periods of importance. Thus, we can assume that the individual components are not defining distinct clusters of variables (stations) that are associated with synoptic anomaly systems. They share variance (except between 2 and 4) from the same regional anomaly areas over the domain, instead of each one defining one distinct pattern of variance.

The spectra studied to find the periods listed above were constructed by summing the eight yearly periodograms for each component, and then averaging the summed periodogram values across three frequencies of each component's periodogram. This resulted in 48 degrees of freedom. The 95 and 99 percent points of the null distribution of squared coherence were computed via the equations

$$1 - (1 - .95)^{1/23} , \tag{31}$$

and

$$1 - (1 - .99)^{1/23} . \tag{32}$$

Table 1. Coherence check between pairs of components being interpreted. Results are significant at the 95% level of confidence for $(coherence)^2 \approx 0.122$

|	$(coherence)^2$					
Component pairs:	1 vs 2	1 vs 3	1 vs 4	2 vs 3	2 vs 4	3 vs 4
Period (Days)						
10.0	.051	.025	.102	.006	.028	.012
9.0	.133	.159	.129	.110	.034	.042
8.2	.134	.161	.063	.123	.013	.048
7.5	.059	.101	.044	.055	.048	.055
6.9	.037	.089	.078	.053	.061	.066
6.4	.110	.143	.047	.042	.096	.161
6.0	.123	.153	.048	.023	.077	.120
5.6	.101	.029	.053	.166	.153	.011
5.3	.440	.073	.002	.114	.140	.115
5.0	.041	.092	.001	.125	.072	.161
4.7	.102	.060	.076	.111	.118	.044
4.5	.122	.138	.144	.010	.111	.119
4.3	.187	.191	.089	.024	.038	.146
4.1	.167	.064	.035	.838	.076	.147
3.9	.045	.037	.089	.106	.173	.069
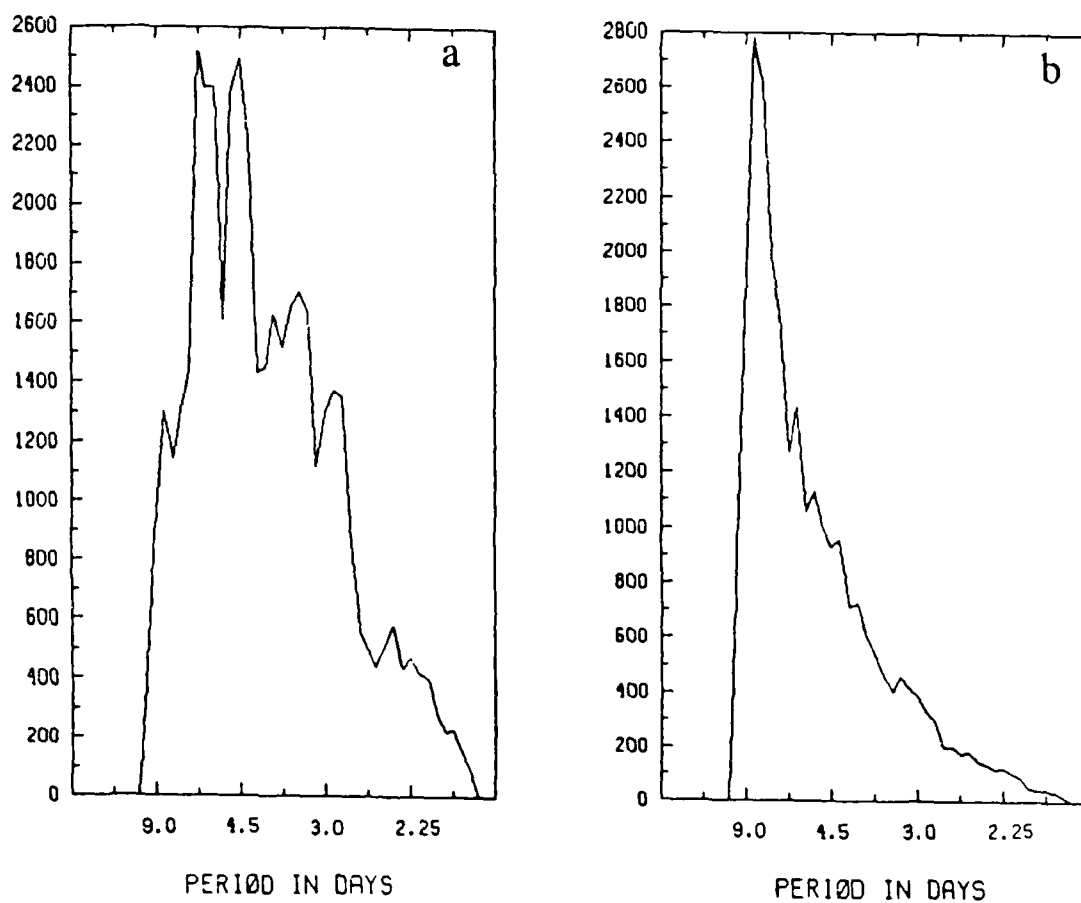
Figure 1. The spectrum for component one (a), component two (b), component three (c), component four (d). Units on vertical axis are millibars squared.
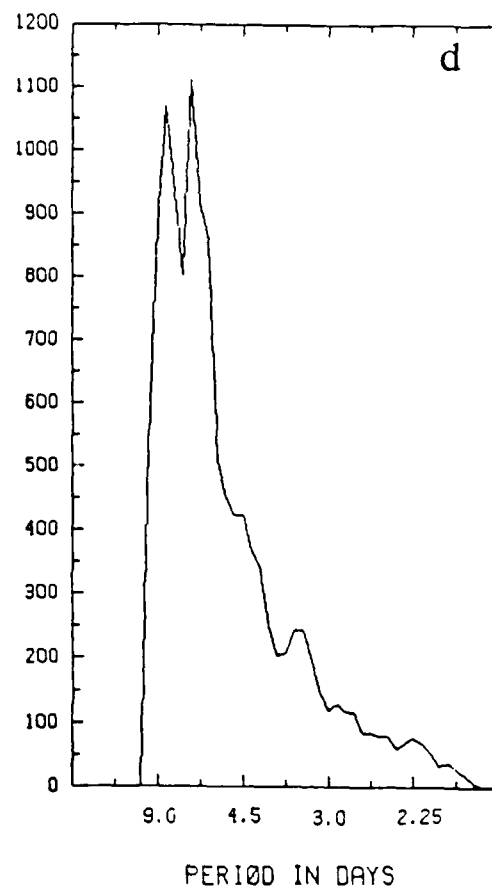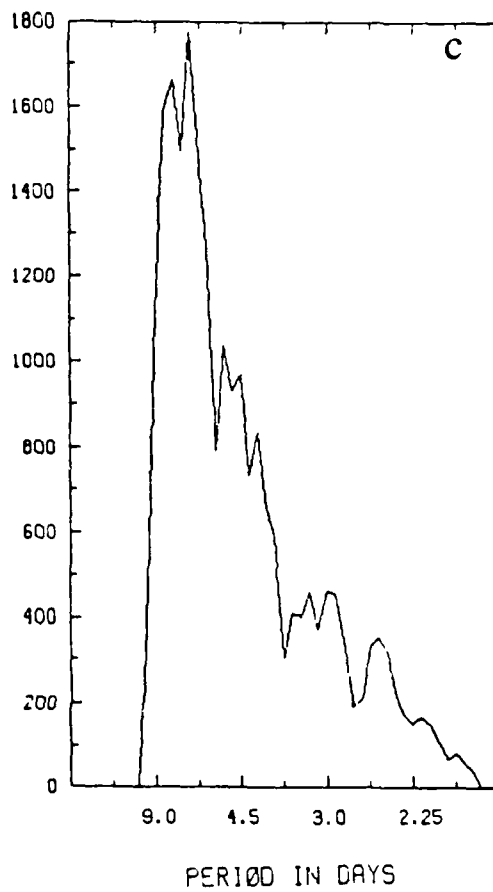
Figure 1. (continued)

5. RESULTS

a. mean SLP and standard deviation

Figure 2a of unfiltered average SLP is very similar to the figure
1a of the same variable by Blackmon et al. (1977) which covers the
years 1963 to 1972 for 15 November to 14 March. Both figures mentioned
above also compare favorably to the mean SLP maps in the Normal Weather
Charts for the Northern Hemisphere.

Figure 2b of the standard deviation of band-passed SLP is very
similar to the figure 2b of the same variable by Blackmon et al. (1977)
for the same time period as mentioned above. A comparison of the
standard deviation plots with the variance of the band-passed 500 mb
heights (e.g., see figure 5a and c of Blackmon, 1976), standard
deviation of the band-passed 300 mb height (e.g., see figure 3b of
Blackmon et al., 1977), and the average wintertime 500 mb vorticity
(e.g., see figure 11 of Blackmon, 1976) reveals some interesting
meteorological connections between the different levels. All the
graphs have maximum values in the area of Nova Scotia and Newfoundland,
with a relative secondary maximum in the area of the Colorado
cyclogenesis region in the average vorticity field of Blackmon's figure
11 (1976). Synoptic experience and past studies (Blackmon et al.,
1984a; Klein, 1967) have indicated that the "average" cyclone tracks
are determined to a large extent by the upper level general circulation
(particularly 700 mb), and should produce a maximum in the pressure
deviations and maximum vorticity at all levels between 40° and 50°N
over eastern North America as the general circulation would tend to
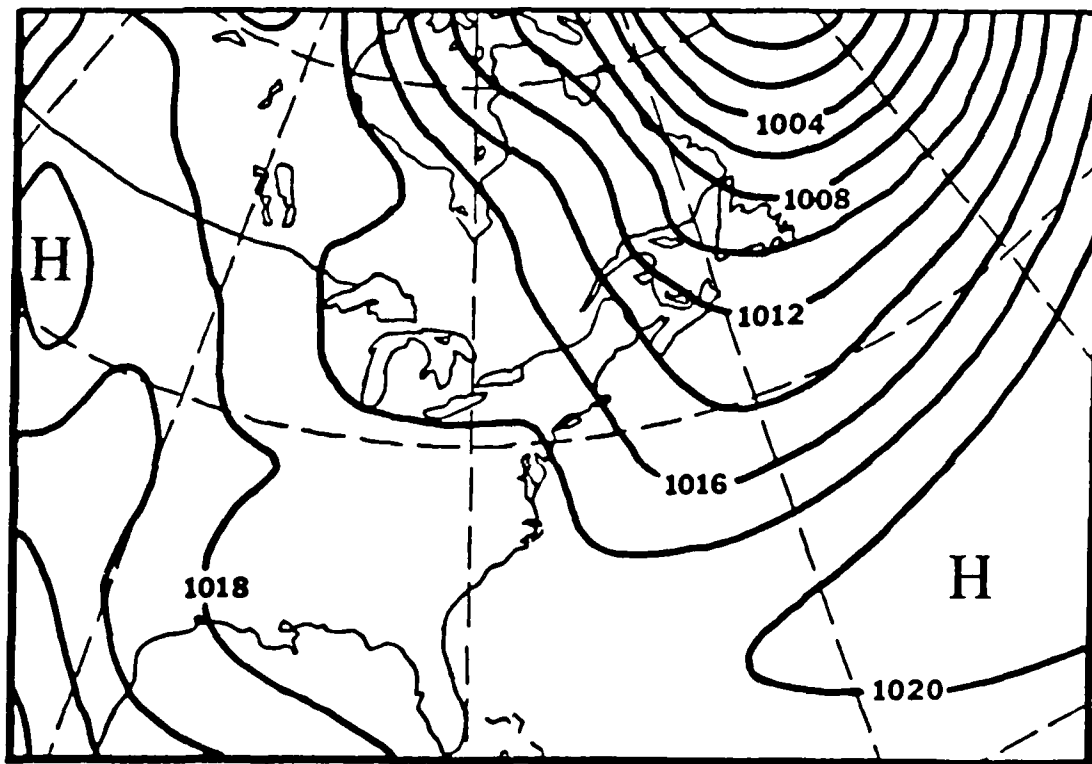guide cyclones to this area. These cyclones are usually mature, deep,

Figure 2a. The distribution of eight-winter average sea level pressure (2 mb interval)
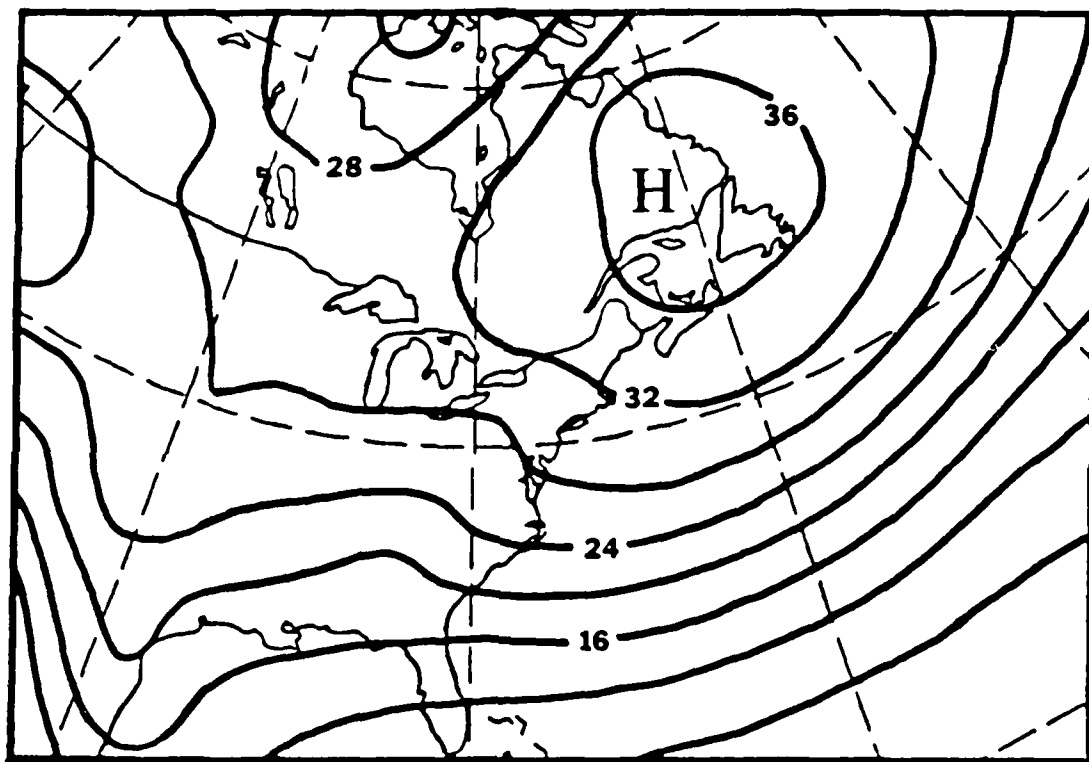
Figure 2b. The standard deviation of sea level pressure for
band-passed filtered, twice daily data (4 mb interval)

and large area covering synoptic scale disturbances. Therefore, the effects of these cyclones should be seen from the surface to the upper levels of the atmosphere (Hartmann, 1974), while the secondary maximum in the 500 mb average vorticity field (e.g., see figure 11 of Blackmon, 1976) is probably induced by the combination of the lee-side cyclonic flow and the maximum cyclogenesis cases per unit area occurring in that area (Whittaker and Horn, 1981).

When looking only at the band-passed SLP standard deviations (figure 2b) the enhanced SLP fluctuations can be seen along the east side of the major mountain ranges caused by cyclonic flow on the lee-side of the ranges. Note how the band-passed SLP standard deviation contours "pinch in" on the main axis of deviations, from the north and south, from approximately 100° to $85^{\circ}W$. Storms moving out of the lee-side cyclogenesis area are usually weak and small in terms of area covered, which will tend to cause smaller deviations in the SLP field, than when they initially had the lee-side circulation support. As they continue to cross the central portion of the United States or southern Canada the cyclones tap moisture and heat sources (Gulf of Mexico or Great Lakes) and begin to intensify, covering larger areas of the earth, and therefore widen and strengthen the standard deviation field of the band-passed SLP. Results of Hartmann (1974), Blackmon et al. (1977, 1979), and Blackmon and White (1982) support the correlation between the standard deviation field in SLP and upper level atmospheric parameters when moving from the highly baroclinic disturbance areas of lee-side cyclogenesis to the less baroclinic, more mature cyclones off the east coast of northern North America.

As noted by Blackmon et al. (1977), a comparison of band-passed SLP standard deviations (figure 2b) with the statistics derived by Petterssen (1956) of the percentage frequency of cyclone centers per unit area during the winter season provides some interesting information. Petterssen's figures 13.6.1 and 13.6.2 show maxima of cyclone centers over the Great Lakes and other warm bodies of water, whereas this study's results and those of Blackmon et al. (1977) indicate only a little enhancement of pressure variability in these areas. This suggests that many of Petterssen's centers over these areas are weak and/or quasi-stationary (Blackmon et al., 1977). This would be analogous to the "pinching" seen in the SLP deviation field as disturbances move out of the lee-side cyclogenesis areas as explained above.

Blackmon et al. (1977) further felt that their variance plot indicated a more widespread region of "lee-side cyclogenesis" downstream from the Rockies. It appears that the band-passed variance plots indicate the movement of cyclones out of the lee-side area as weak cyclones, causing "pinching" in the SLP deviation field before they begin to later intensify and expand in area as they head toward the east coast of North America. As stated by Blackmon et al. (1977), the work of Reitan (1974) closely resembles the band-passed SLP standard deviation field, which it should since the cyclones tend to follow the longwave circulation and trace out a pattern of increasing pressure variance as they intensify and grow in areal size. Reitan's (1974) figure 12 further confirms that the cyclone tracks to the lee-side of the Rockies all converge in the Nova Scotia-Newfoundland

area, as would be caused by the mean upper level flow (e.g., see figure 2 of Blackmon et al., 1984b).

The results of Blackmon (1976), Blackmon et al. (1977, 1979, 1984a), and others mentioned in this section agree with the average and standard deviation of SLP plots (figures 2a and b) of this study. It doesn't appear the data set being considered in this study is abnormal. The results of the CPCA should give a good idea of the normal areas of preferred synoptic scale disturbances and their movement.

b. component number one

The first component of the CPCA accounted for approximately 26.6 percent of the variance in the band-passed filtered data set. The period of the most important wave structures contributing to the spectrum of this component were estimated to be 4.5 to 5.0 days and 5.6 to 6.4 days.

1) spatial properties

Figure 3a is the spatial amplitude plot of the first component. There is one main area of variability centered over northern Nova Scotia with a ridge of variability extending to the NE along 50°N, and also extending to the SW to a secondary maximum over northern Oklahoma. There are two areas of lower variability evident, the first being the area over the Atlantic Ocean near 21°N, 50°W, which should be associated with the subtropical anticyclone in this area. There is an extension of this area along the Gulf Coast and up the west side of the Appalachian Mountains. The second area of lower variability is located over the western Hudson Bay area extending down to the western Great
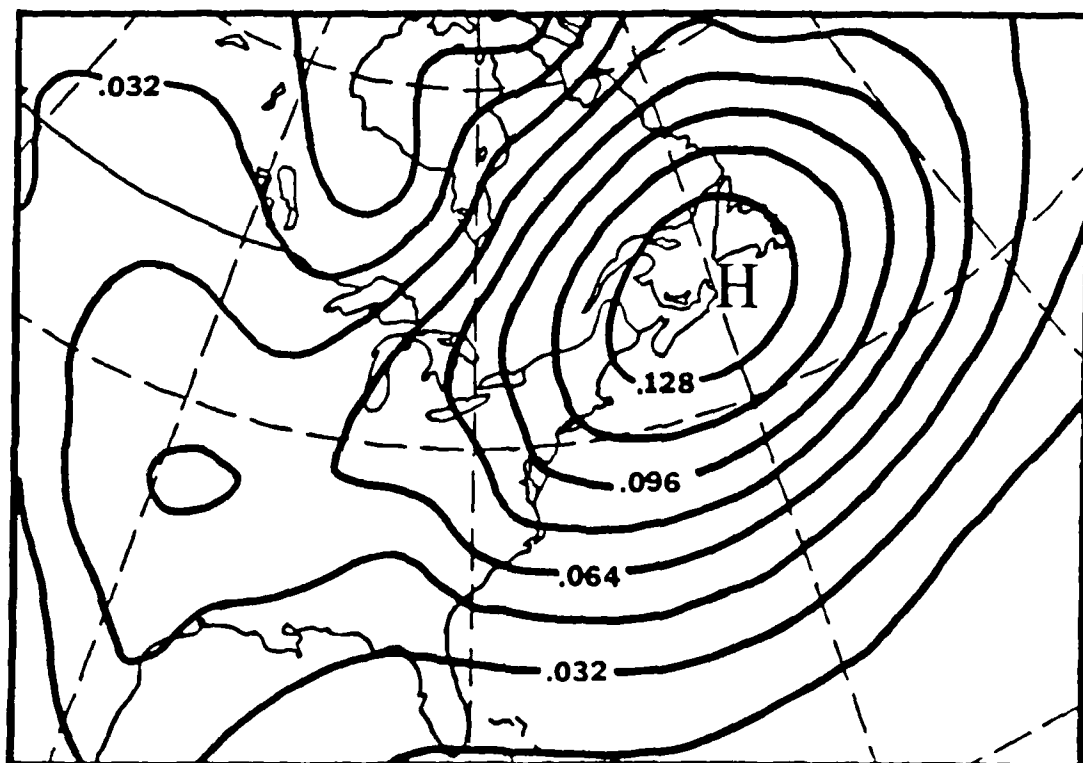
Figure 3a. The spatial amplitude (relative units) for component one
of the band-passed filtered data

Lakes. This area appears to be induced between the higher variability areas of the lee-side of the Rockies and Nova Scotia.

The spatial amplitude plot closely resembles the average wintertime 500 mb vorticity pattern (e.g., see figure 11 of Blackmon, 1976). The area of maximum values in both plots over Nova Scotia agrees well with the idea that cyclones that reach this area are mature, deep disturbances affecting much of the atmosphere vertically (Blackmon et al., 1979; Hartmann, 1974). A look at the plots of 500 mb geopotential height variance (e.g., see figure 5c of Blackmon, 1976) and 300 mb height standard deviations (e.g., see figure 3b of Blackmon et al., 1977) of band-passed data also observationally supports the idea of mature cyclone structures near Nova Scotia.

The area of maximum variability in figure 3a is also located to the north side of the winter average 500 mb zonal wind speed maximum (e.g., see figure 6a of Blackmon et al., 1977). This location is in agreement with Palmen and Newton (1969), who found that as cyclones mature the sea level circulation center deviates increasingly to the left of the jet stream.

White (1980) plotted the ratio of band-passed wintertime 500 mb geopotential height variance contribution of long waves to synoptic scale waves. White's figure 2 shows a distinct minimum in the ratio over the Nova Scotia-Newfoundland area, where component one has maximum variability due to synoptic scale activity. This ratio minimum shows that the long waves are contributing very little to the variance in the 500 mb geopotential height, further supporting the importance of synoptic scale activity in the Nova Scotia-Newfoundland area.

Figure 3b is the spatial phase plot for component one. The relative phase angles increase from west to east, indicating eastward movement of the fluctuations in the SLP field. The more widely spaced isolines of phase angles (in units of degrees) in the lee-side of the Rockies indicates the faster movement of these young, weak disturbances as they move in a southern direction before turning eastward. After turning eastward the phase angle isolines in the northern portion of the United States indicate a relative decrease in the area covered between changes in isoline values. This appears to indicate a relative speed decrease in the movement of the disturbances in the northern United States. Meanwhile, in the southern portion of the United States the phase angle isolines appear to indicate the relative speed of the disturbances has not slowed down as much as they have in the northern United States, until they start being influenced (blocked) by the Appalachian Mountains. The disturbances in the northern United States appear to speed up once they reach the Great Lakes area, and all disturbances appear to increase in speed once they come under the influence of the warm Atlantic Ocean waters, especially in the area of the Gulf Stream. One possible explanation for this speed increase would be that the disturbances are receiving energy from the warm waters of the Great Lakes, Gulf of Mexico, or Atlantic Ocean. More work needs to be done to support this explanation. The question to be answered is, do disturbances in fact speed up, on a consistent basis, when energy is input? It also appears from the plot that once the disturbances move east of $60^{\circ}W$, they move at a fairly regular speed.
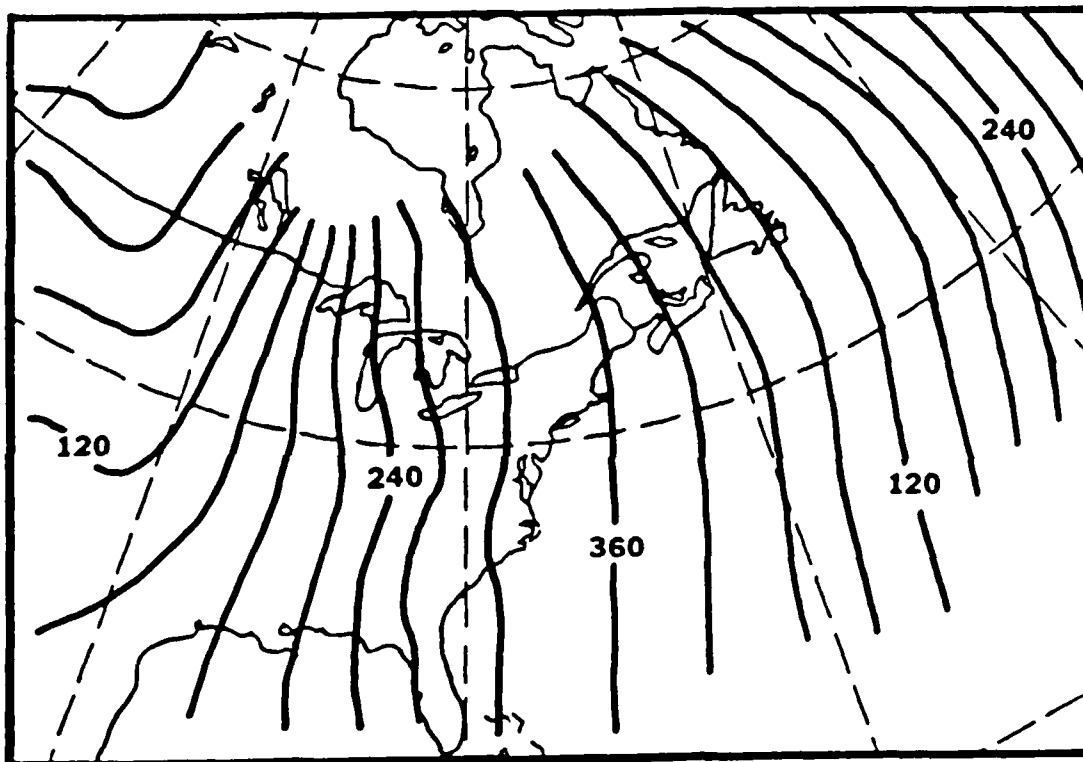
Figure 3b. The spatial phase (30 degree interval) for component one of the band-passed filtered data

These disturbances should be mature, fully developed systems, which have reached a fairly steady state of energy input.

The structure of the phase angle isolines in figure 3b correspond closely to the structure of the patterns of correlation values of 500 mb height deviations which exhibit a west to east oriented wave-like structure, with a zonal wavelength of about 4000 km, as reported by Blackmon et al. (1984a). The results of Blackmon et al. (1984a) indicate that these short-time scale (2.5 to 6.0 days) fluctuations are aligned slightly poleward and downstream of the climatological mean jet stream speed maximum and with axes oriented along the climatological mean flow. The fluctuations which produce these correlation patterns also have a predominant zonal scale of wavenumber 6-7, and are clearly related to baroclinic eddies (synoptic scale disturbances) as discussed by Blackmon (1976) and Blackmon et al. (1977).

It appears the 700-500 mb mean wind flow pattern is creating the phase angle pattern shown in figure 3b. An examination of the mean wintertime 700 and 500 mb flow, and the results of Klein (1967) and Blackmon et al. (1984b) all support the idea that the "average" variance pattern in SLP is traced out by the upper level mean flow pattern. Further support is given by the work of Bowie and Weightman (1914), Reitan (1974), and others showing the convergence of preferred storm tracks into the area near Nova Scotia after having followed paths across North America that approximate the mean upper level flow pattern.

2) temporal properties

Figure 3c is the temporal amplitude plot, by year, for component one. The plot shows that component one was weakest in 1981 and strongest in 1973. This can be seen by looking at the squared temporal amplitude (variance) in table 2 also.

The monthly weather summaries in Weatherwise and the Climatological National Summary suggest that 1973 was the most active year (of the eight studied) of cyclone activity, with the 700 mb jet displaced south to the gulf coast. On the other hand, 1981 was a year with a blocking ridge along the west coast and a trough along the east coast causing a large number of storms to form and intensify as they moved off the coast of Nova Scotia. Therefore, they did not contribute a great deal to the "overall" pattern of component one.

Figure 3d is the temporal phase plot of component number one which shows that it is dominated by disturbances whose phase changes with a fairly quick, linear progression. Only a few stand out as being slower progressing features. But these did not contribute significantly to the variance of the component as can be seen by comparing the temporal amplitude plot to the temporal phase plot at the time of occurrence of the more slowly progressing features.

3) comments

Component one seems to represent the pattern produced in the pressure variance field by disturbances moving roughly with the mean mid-tropospheric flow. Care must be taken that the variance is not described only in terms of cyclone activity. Petterssen (1956) describes the "cyclone family" as consisting of both a train of
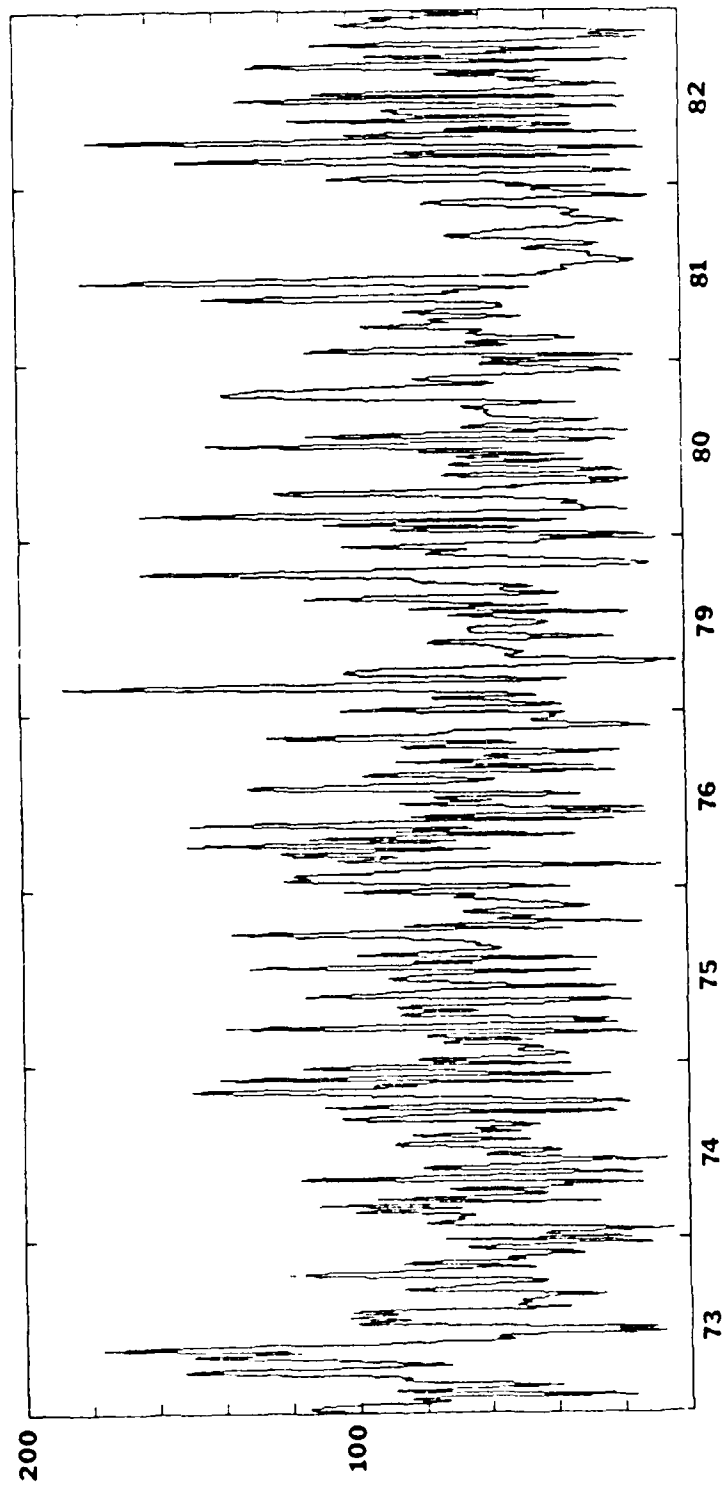
43

Figure 3c. The temporal amplitude (interval of 20 mb) of component one of the band-passed filtered data, by year
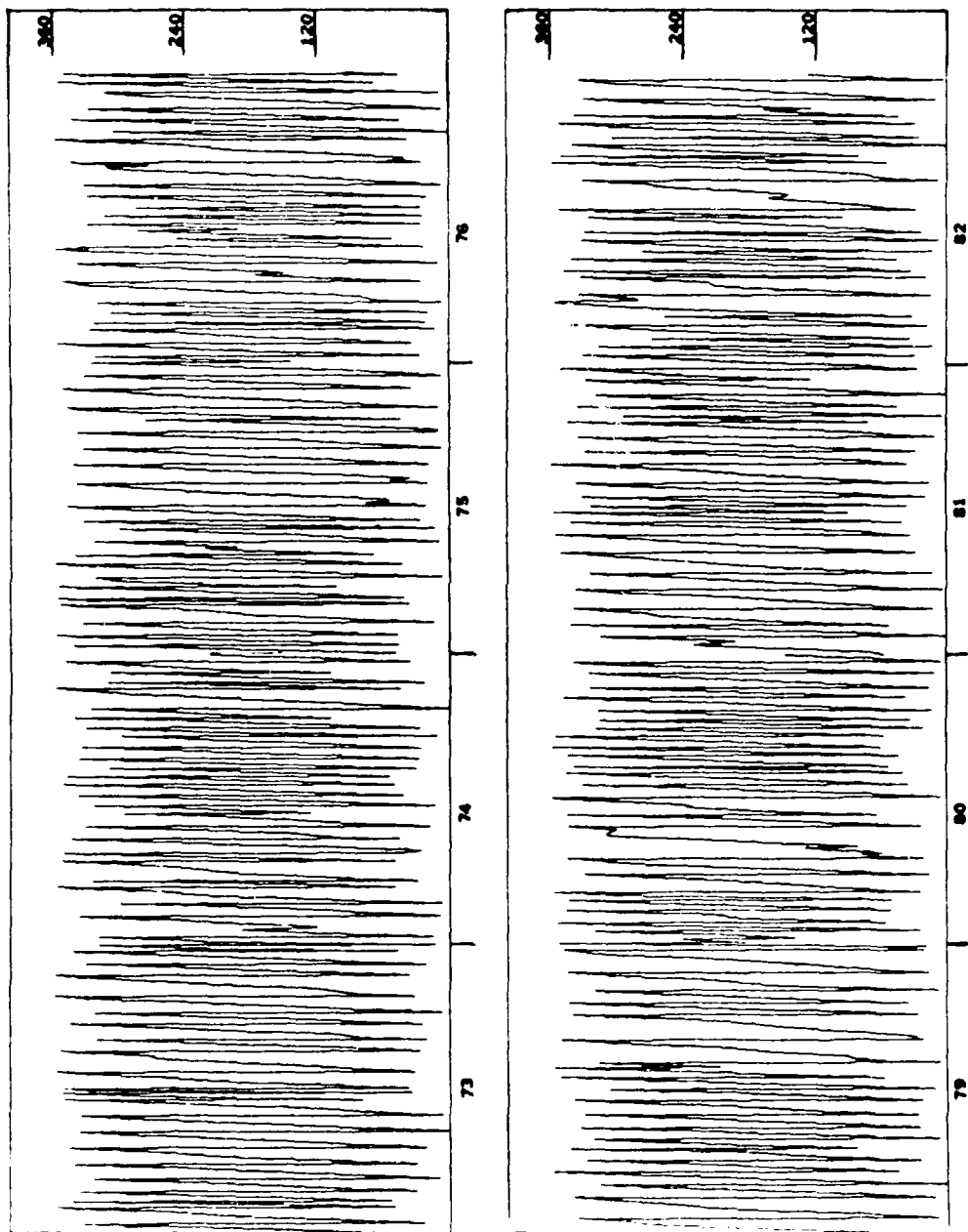
44

Figure 3d. The temporal phase (degrees) of component one of the band-passed filtered data, by year

Table 2. Squared temporal amplitude (variance), by year, for each
component in units of squared millibars

	variance (mb)^2							
Year:	73	74	75	76	79	80	81	82
Comp. 1	7155	5279	5146	6393	5458	5289	4286	6012
Comp. 2	3317	3812	3138	4490	2916	2730	2863	3491
Comp. 3	3536	2387	2516	3775	2405	2515	2582	3434
Comp. 4	1622	2203	1434	1649	1711	1578	709	1479

cyclones and anticyclones (e.g., see figure 12.5.1 and 12.5.2 of Petterssen, 1956). The anticyclones, as noted by Petterssen (1956), appear quite often to be sluggish, passive systems that fill the space between active cyclone systems. This seems to fit in well with the occasional more slowly changing phase angle of some events in the temporal phase plot. Klein (1958) found that the average life span for all pressure centers was approximately five days, with anticyclones usually lasting one day longer than cyclones.

c. component number two

The second component accounts for approximately 15.8 percent of the variance in the band-passed data set. The period of the most important wave structure contributing to the spectrum of this component was estimated to be 8.2 to 9.0 days.

1) spatial properties

Figure 4a is the spatial amplitude plot for component two. There is one maximum area of variability over the Dakotas and Minnesota with extensions of this area along ridges of variability southward to the Texas gulf coast, northward into Alberta, and ENE through Canada along and just north of 50^ON latitude. There appears to be a relative secondary maximum in the variability off the Atlantic coast centered near 35^ON, 64^OW. The two areas of relative minimum variability are located over Florida, and near 43^ON, 53^OW.

The spatial amplitude pattern maximum over the Dakotas and Minnesota matches closely the area of maximum frequency of anticyclones centers found by Miller (1932), Zishka and Smith (1980), and Klein
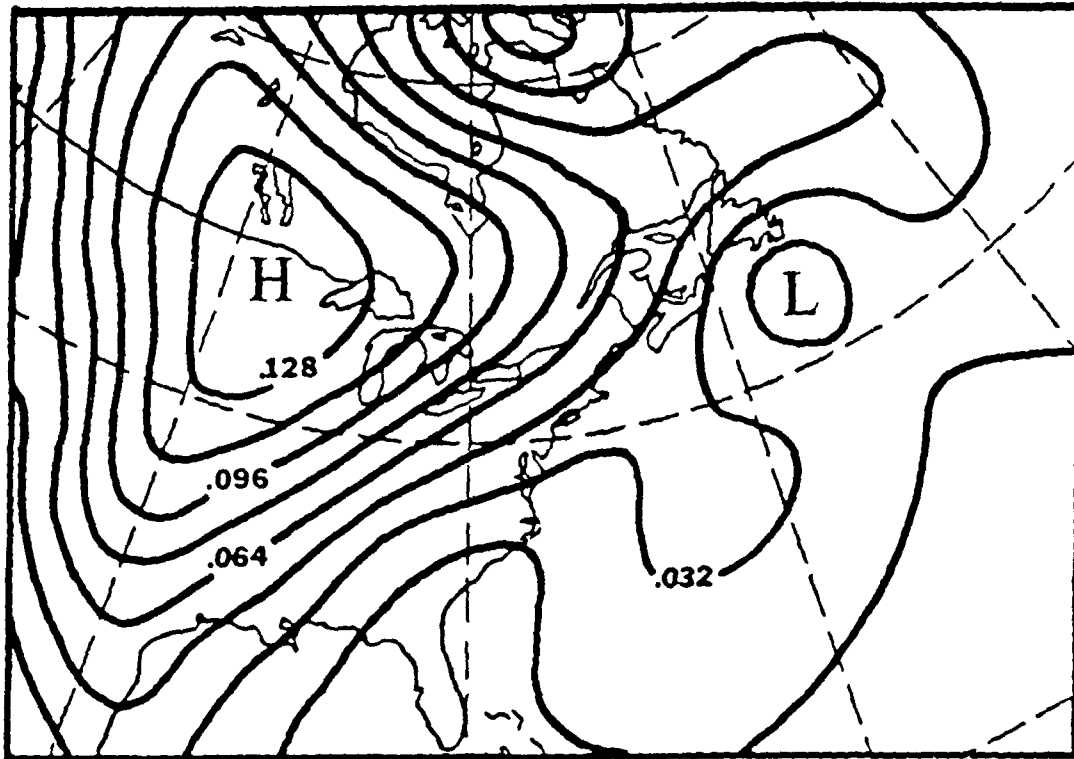
Figure 4a.   The spatial amplitude (relative units) for component two
of the band-passed filtered data

(1957). The extensions of this area to the south and ENE follow closely the preferred tracks of anticyclones as reported by Zishka and Smith (1980), Wasko (1954), and Klein (1957).

A look at the actual cyclone and anticyclone tracks, for the eight years studied, shows the area along the United States-Canadian border was a very frequent path used by these disturbances. Further, there were a number of anticyclones that moved southward into the central portion of the United States.

An examination of figure 9b of Blackmon et al. (1977) of band-passed 850 mb temperature standard deviation reveals that this plot and figure 4a of this study are nearly identical in shape. The area of maximum variability in the SLP to the east of the Rocky Mountains and the area of maximum deviation in the 850 mb temperature plot of Blackmon et al. (1977) could possibly be linked to the outbreak of shallow, modified, polar air into the central United States, just east of the Rockies, during the winter season. These cold air outbreaks can, and do, reach as far south as Texas and Mexico (Blackmon et al., 1979). The graphs of Blackmon et al. (1979) of the correlation between the 1000 mb and 500 mb height (their figure 3b) and between 1000 mb height and the 1000-500 mb thickness (their figure 12) supports the idea that the outbreaks are relatively shallow and do not extend up to the 500 mb level in the atmosphere. The increase in pressure at the surface is compensated for by the decrease in temperature in the lower atmosphere, so the effects of the polar air are not seen at the upper levels of the atmosphere. A look at surface temperature anomalies for

the period of study shows departures from normal as much as 12 to 18
degrees Celsius below normal over the west-central United States.

The area of low variability over Florida is probably present due
to the subtropical high being in control of the area most of the time.
The other low variability area is probably induced by the CPCA
technique. As mentioned in section 4, since component one had a large
variability center over Nova Scotia, the low variability at 43^ON, 53^OW
in component two could be induced by component one's pattern.

Figure 4b of the spatial phase plot for component two shows the
movement of the fluctuations has two main paths. Both paths as in the
start in Canada around 58^ON, 116^OW and travel SSE toward the united
States. One path continues into the United States, heading toward
Texas and the gulf coast, while the other breaks off and heads east
along the 50^ON latitude circle. The path into the United States and
toward Texas matches well with the idea of cold air outbreaks. The
other path, along the 50^ON latitude circle, matches with the idea of a
major anticyclone/cyclone path through this area as shown by Klein
(1958) and Wasko (1954).

2) temporal properties

The temporal amplitude plot, figure 4c, for component two shows
that 1976 was the year in which the contribution of the second
component to the total variance was a maximum, while 1980 contributed
the least (see table 2 also). In 1976 the mean 700 mb trough was
shifted westward and centered over the Great Lakes. This shifted
orientation would tend to direct disturbances southward on the west
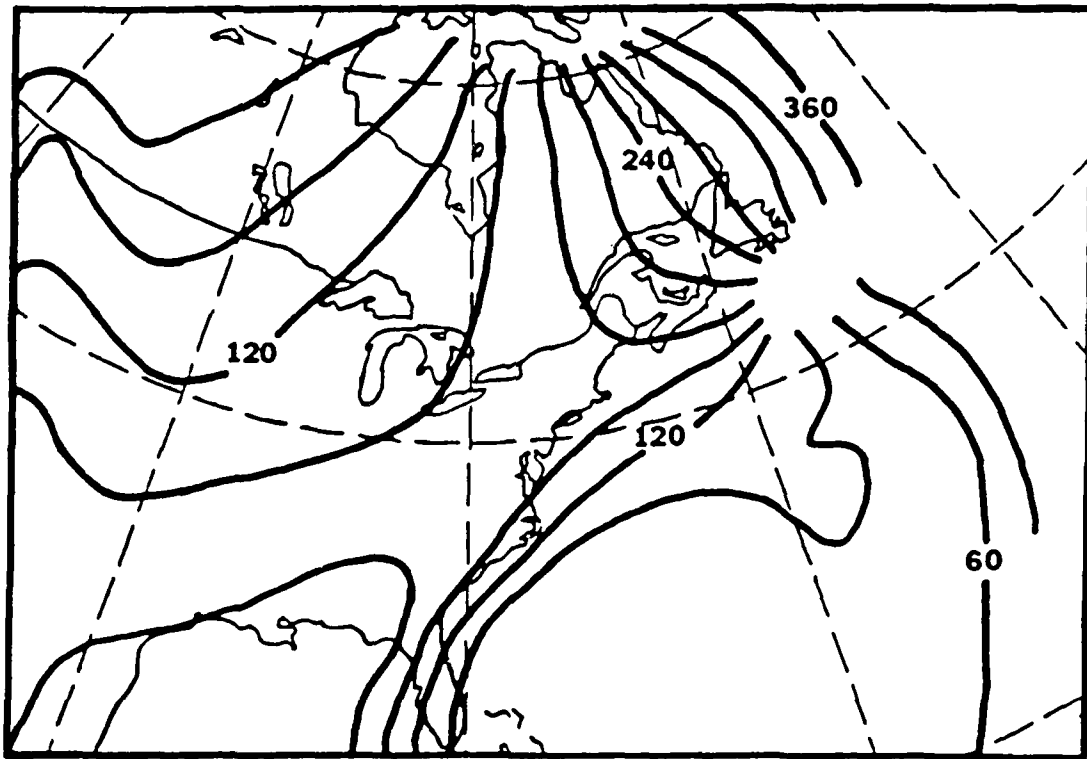side of the trough through the Great Plains area more than usual.

Figure 4b. The spatial phase (30 degree interval) for component two of the band-passed filtered data
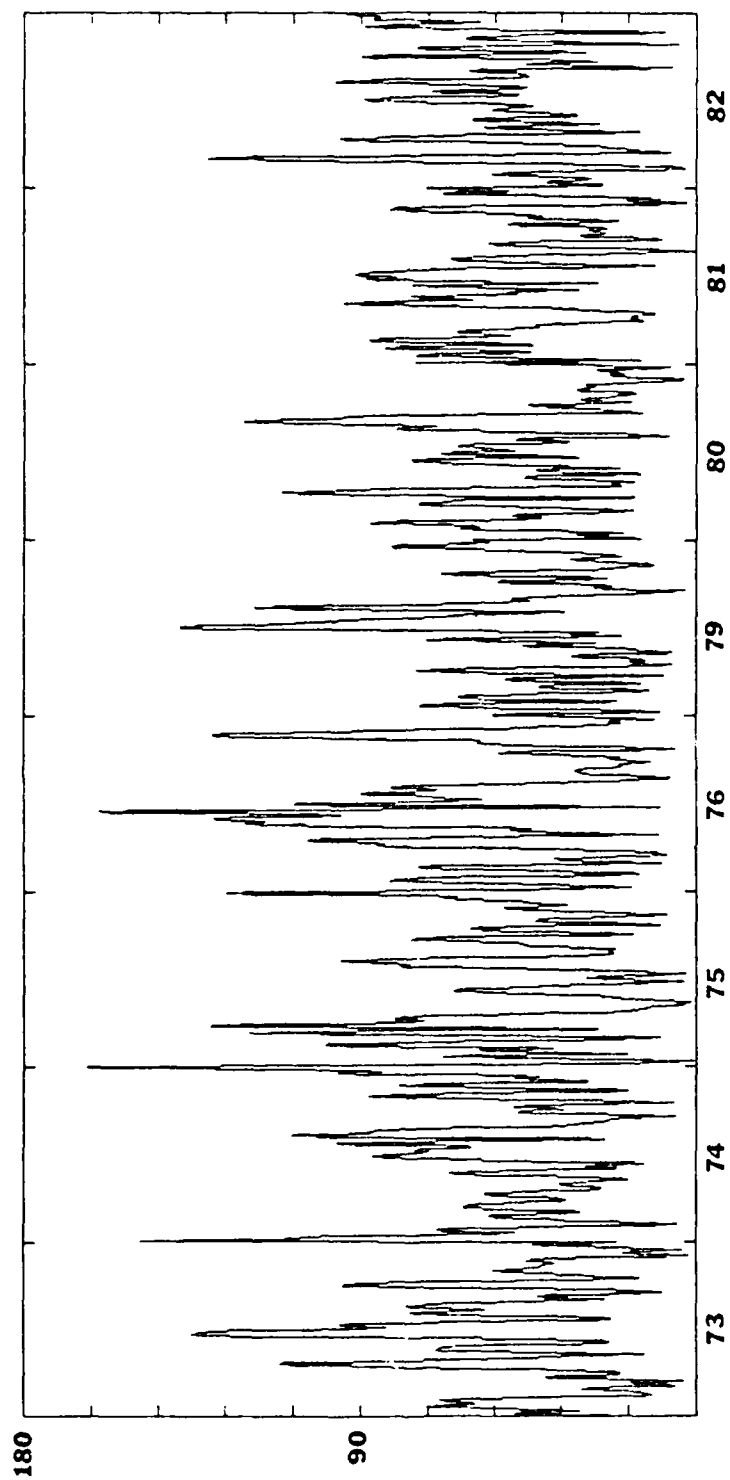
Figure 4c. The temporal amplitude (interval of 18 mb) of component two of the band-passed filtered data, by year

While in 1980, the west-central United States experienced a warmer than usual winter. There were few cold air outbreaks moving southward out of Canada.

The temporal phase plot (figure 4d) reveals that the phase is changing more slowly with time, for the most part, than it did for component one (figure 3d). This is in keeping with the idea of more slowly moving anticyclones dominating this component with some slower moving cyclones probably mixed in.

3) comments

This component seems to be associated with cyclones which are taking a northern track due to possibly a strong anticyclone over the eastern United States and anticyclones that track along the United States-Canadian border. It is also linked to the cold air outbreak anticyclones that track southward just to the east of the Rockies. These outbreaks seem to be enhanced by a trough in the upper level circulation over the Great Lakes.

The coherence check (table 1) shows that this component is correlated with component one, especially in the 8.2 to 9.0 day period. This seems to indicate the cold air outbreaks may add to the variability of both components, just to the east of the Rockies, due to the time length of the significant period which would indicate slower moving anticyclones.

d. component number three

The third component accounts approximately for 13.7 percent of the variance in the band-passed data set. The periods of the most
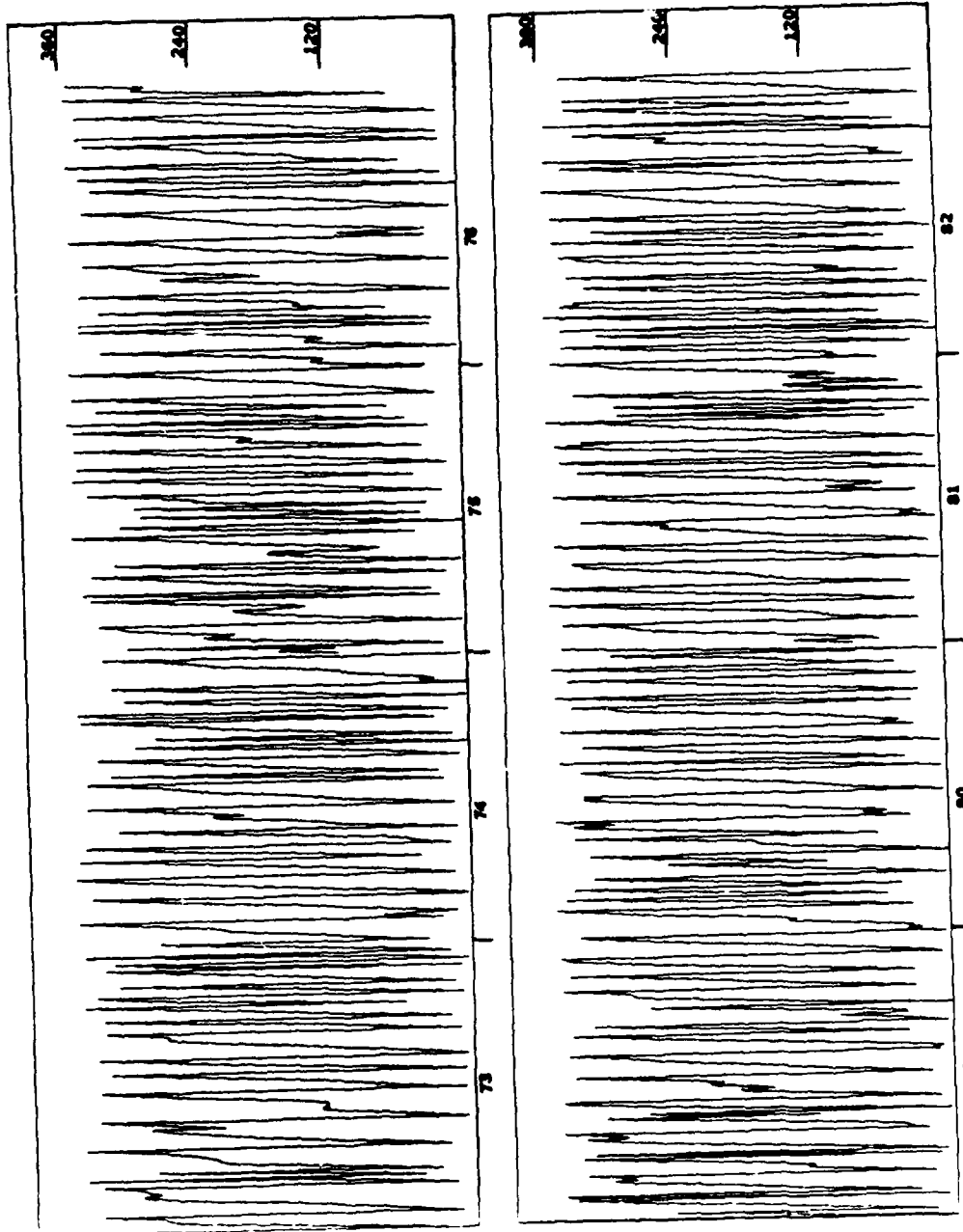
Figure 4d. The temporal phase (degrees) of component two of the band-passed filtered data, by year

important wave structures contributing to the spectrum of this component were estimated to be 6.4 to 9.0 days.

1) spatial properties

Figure 5a is the spatial amplitude plot for the third component. There are two areas of maximum variability separated by a line of low variability through the central plains states.

The area of variability over the Rocky Mountains extends out of Alberta, Canada, down to the Gulf of Mexico, but has its center in the central Rockies over northern Utah and southwest Wyoming. This area corresponds very closely to a maximum area of anticyclone events and anticyclogenesis as depicted by Petterssen (1956, figures 13.7.1 and 13.7.2) and Zishka and Smi'h (1980). The pattern is also located in one of the areas of high alternation between cyclones and anticyclones in the winter season (e.g., see figure 13.8.2 of Petterssen, 1956). Petterssen (1956) speaks of polar outbreak highs moving along the west coast. This component seems to represent these outbreaks somewhat, while component two seems to represent the polar-outbreak highs over the central plains states.

The second area of variability centered over the Coast of Labrador has two southward curving extensions: one extends to the SW to the Great Lakes, and the other one extends to the SE to 49°N, 47°W, and from there it curves back to the SW through 40°N, 50°W. This area seems to fit the cyclone tracks depicted by Reitan (1974) and Zishka and Smith (1980) for the area extending back to the Great Lakes from the center over the Coast of Labrador. But the area extending off the Atlantic Coast appears to have too much curvature back to the NW after
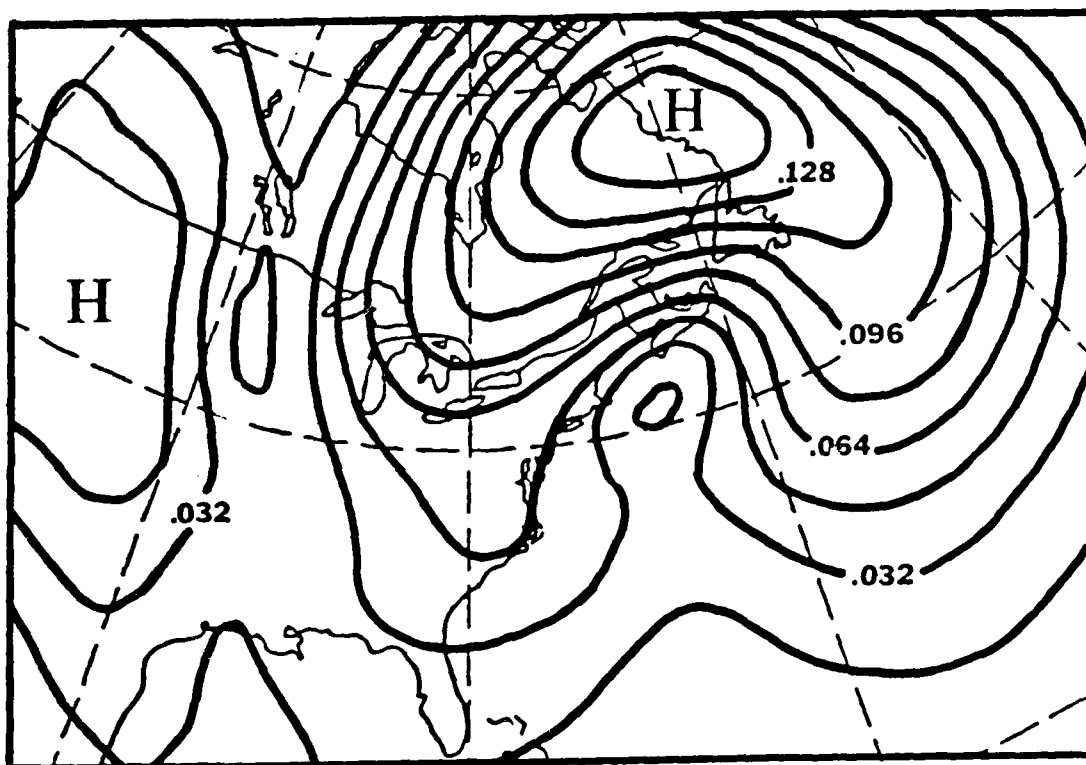
Figure 5a.   The spatial amplitude (relative units) for component three
of the band-passed filtered data

passing the tip of Newfoundland, to match very well with published cyclone tracks.

The extension of the area of variability off the Atlantic Coast seems to be artificially forced to curve due to the induced area of low variability near 42°N, 68°W. This low variability area appears to be present due to the extremely high variability area near this location in component one. Since component one accounted for a large part of the variability in this area, component three has low variability there because component three accounts for the variability left in the data field after the variability due to components one and two has been taken out. There is also the possibility that the shape of the variability area is caused by the domain problem as noted in section four. Climatological storm track data show that one of the primary tracks for storms leaving the Great Lakes area is to the NE through Quebec and the St. Lawrence River area. At the same time, storms moving around the eastern side of Nova Scotia will join the Great Lakes storms in the area off the Labrador Coast and then all of them move off to the east of Greenland. The boundary of this study's domain is very close to this storm convergence area off of the coast of Labrador, and may cause the sharper than normal curvature of the paths of the storms, as suggested by the variability pattern.

Figure 5b is the spatial phase plot for component three. The change in the relative phase angles over the western part of the plot shows a progression in the fluctuations from north to south. Meanwhile, the variability area centered over the coast of Labrador has phase angle shifts feeding in from the Great Lakes area and from off
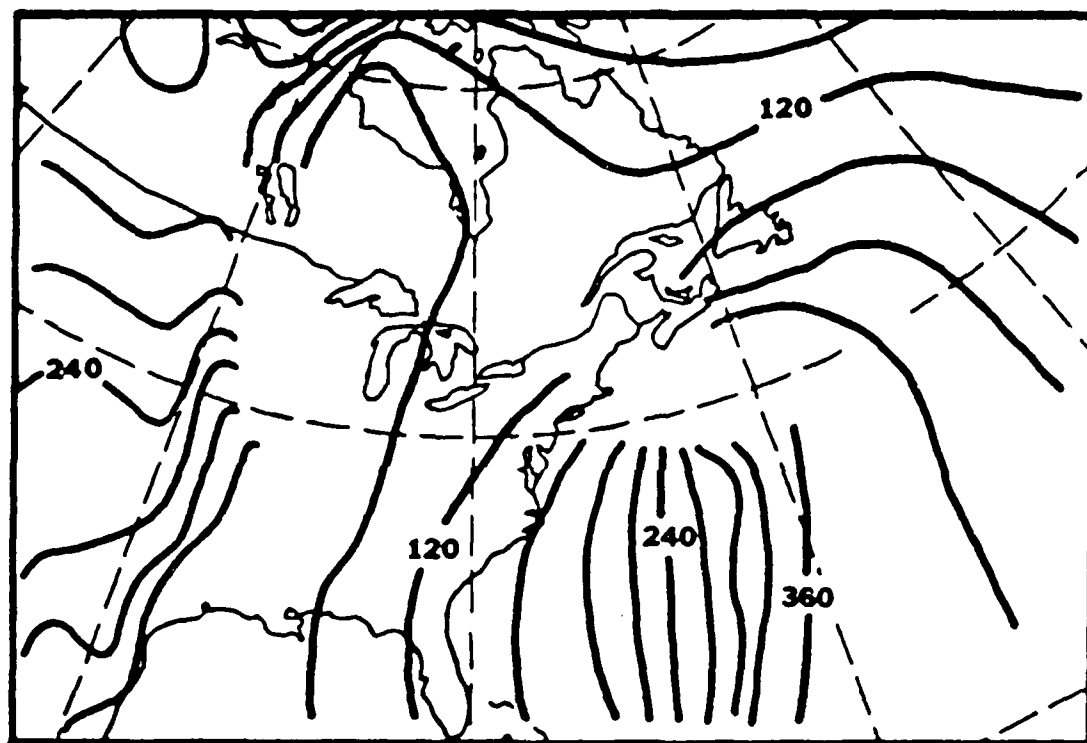
Figure 5b. The spatial phase (30 degree interval) for component three of the band-passed filtered data

the Atlantic Coast around Newfoundland, meeting near 60^ON, 60^OW, in phase, and then moving off to the north.

Over the areas of low variability there is a general west to east propagation of the fluctuations (similar to component one). These fluctuations are in phase with the two main areas of variability. This is understandable since all of these spatial patterns are connected to the general circulation pattern, while there are areas that exhibit greater spatial variability in pressure than others.

2) temporal properties

Figure 5c is the temporal amplitude plot for component three. Table 2 shows that component three was strongest in 1976 and the weakest in 1974. The year of 1976 is also the most active year for component two. The fact that components two and three are most active in the same year is not surprising since they both seem to represent polar-outbreak events, just in different spatial areas. The Rocky Mountains seem to be the dividing line between the two areas.

Figure 5d is the temporal phase plot for component three. It shows that component three is composed of a combination of fairly rapid, linear change of phase events, and slower, sometimes nonlinear change of phase events. This fits in well with the idea of two different types of events making up this component--the faster moving cyclones over the northeastern portion of the domain and slower moving anticyclones over the western portion of the domain.
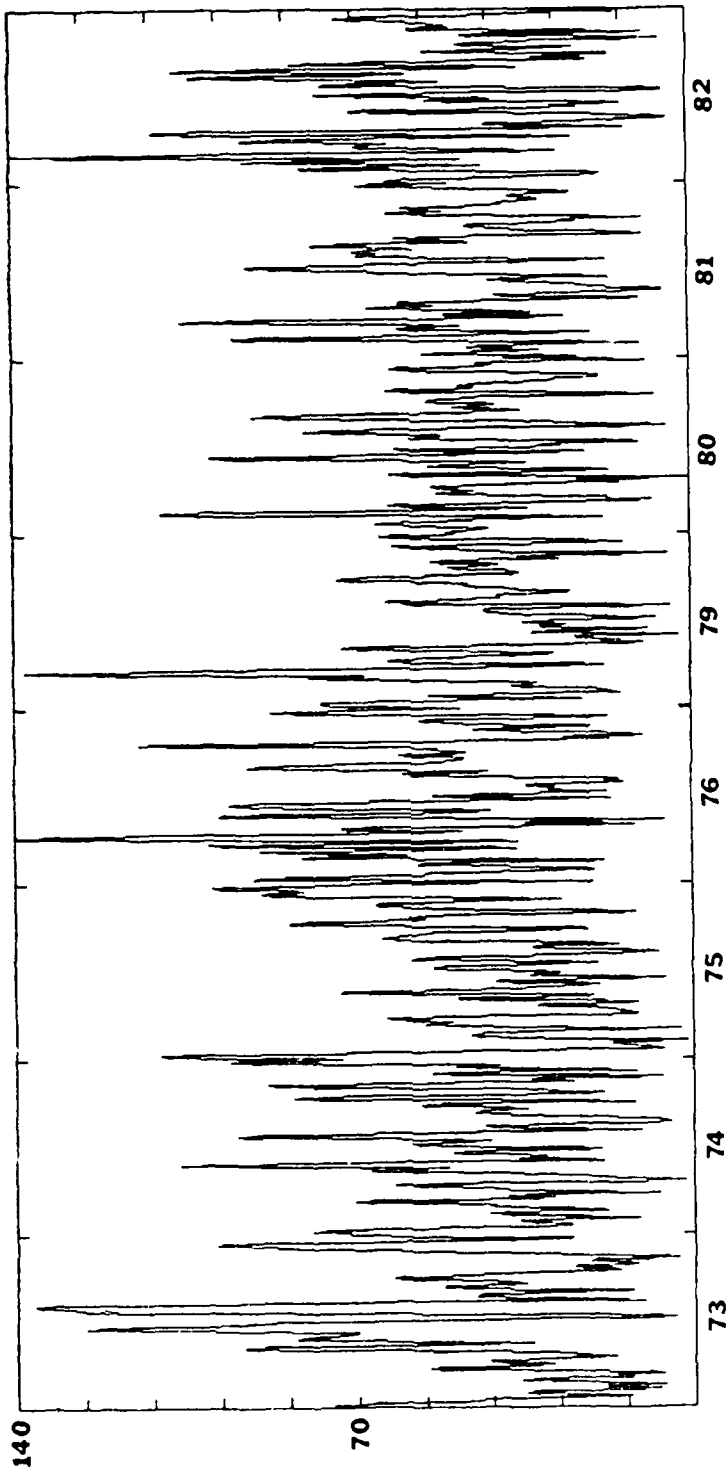
Figure 5c. The temporal amplitude (interval of 14 mb) of component three of the band-passed filtered data, by year
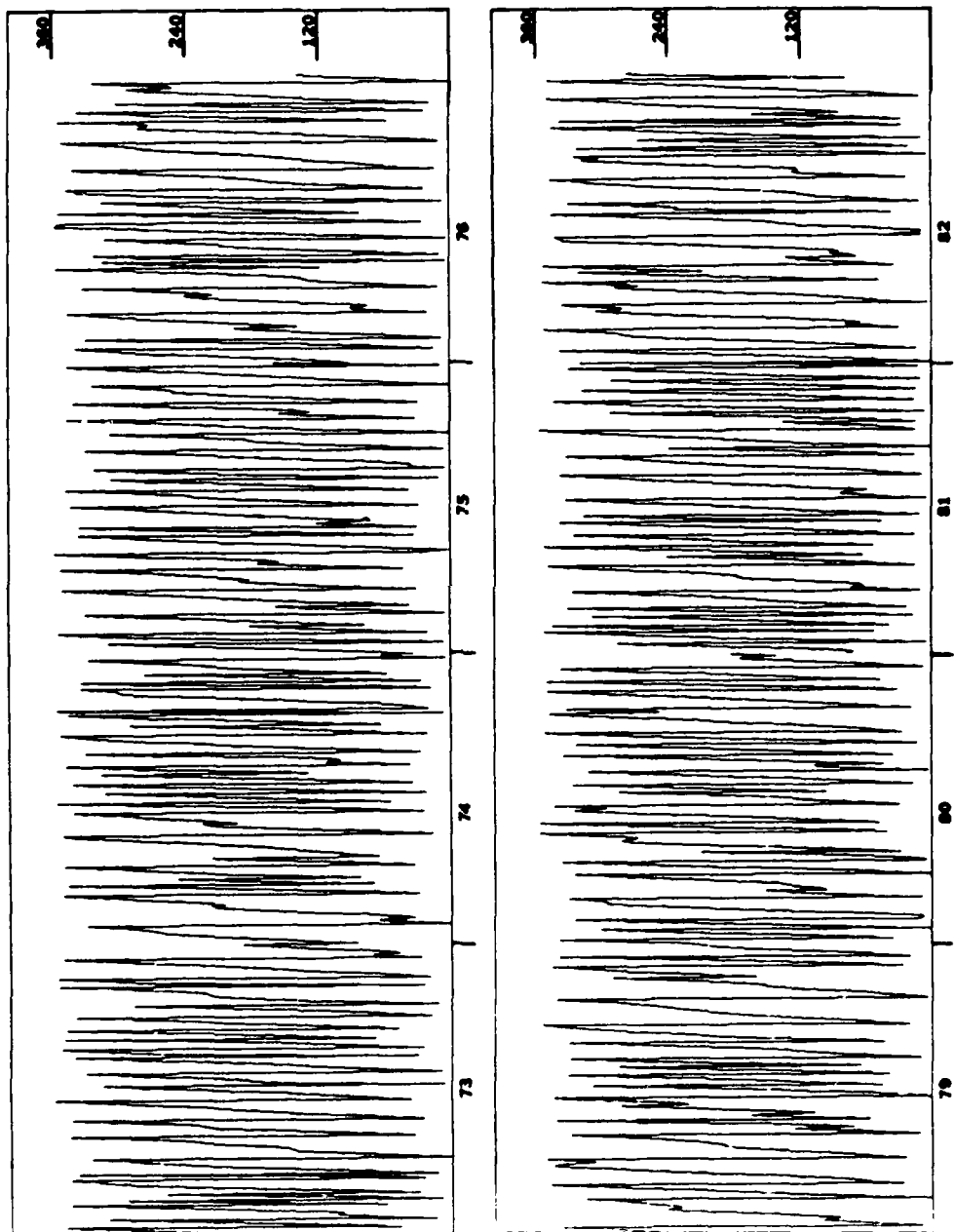
Figure 5d. The temporal phase (degrees) of component three of the band-passed filtered data, by year

3) comments

This component proves to be the hardest to interpret. It appears
to be composed of two spatially distinct events that cover a time
period of 6.4 days to 9.0 days. The western variability area is weaker
than the eastern one, but seems to be more easily interpreted than the
eastern one.

The coherence check (table 1) shows that there is a significant
amount of coherence between component three and the other three
components being studied. We can detect the presence of component one
in component three if we concentrate on the low variability areas in
the spatial phase function of component three, i.e., general west to
east shift. The north to south movement to the west of the Rockies has
some movement over the Rockies as does component two, so it's not a
clear separation of the two areas.

e. component number four

This component accounts for approximately 7.3 percent of the
variance in the band-passed data set. The periods of the most
important wave structures contributing to the spectrum of this
component were estimated to be 6.9 and 9.0 days.

1) spatial properties

Figure 6a is the spatial amplitude plot of component four. It has
two main areas of variability, the first being centered over the
eastern portion of Hudson Bay and the northern portion of Quebec. This
area's variability is almost equal to the variability of the other area
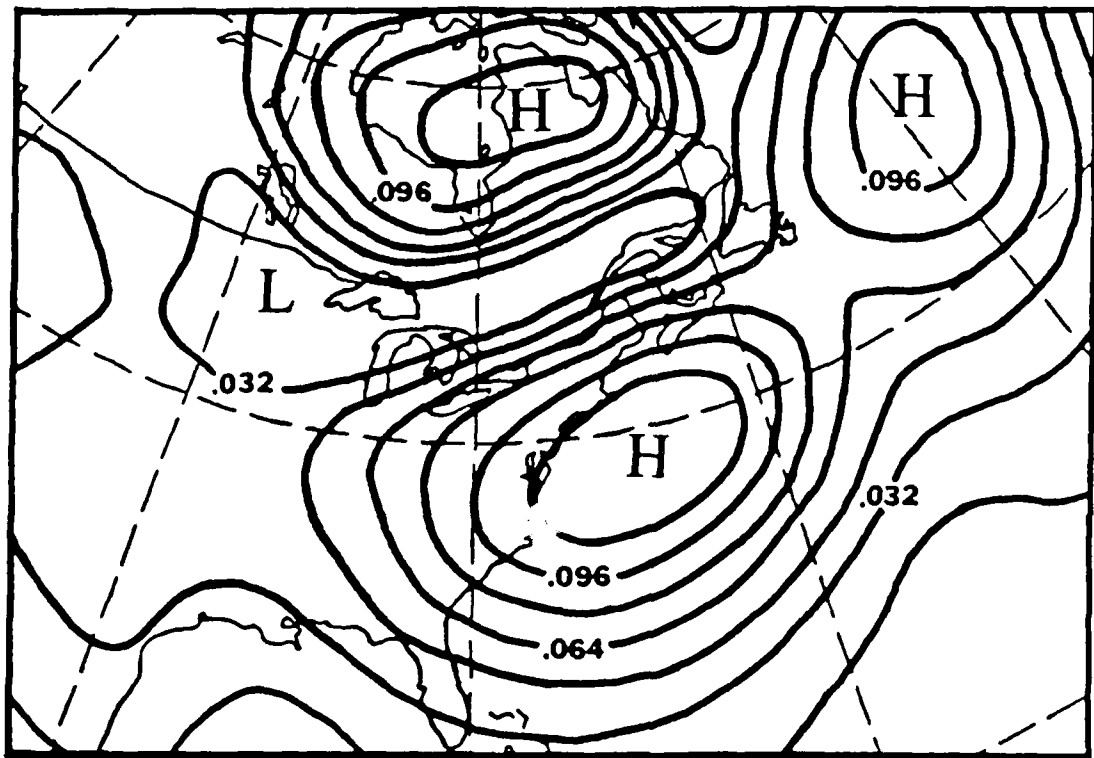present and separated from it by an area of low variability. This

Figure 6a.   The spatial amplitude (relative units) for component four
of the band-passed filtered data

second area of maximum variability has a double center: one located near 40°N, 70°W, and the other near 50°N, 40°W. These two centers are part of an elongated area whose axis extends from Arkansas through North Carolina and Virginia, and then out along the Atlantic Coast through the two centers mentioned above.

This second area off the Atlantic Coast has a close resemblance to the "bomb" deepening area as reported by Roebber (1984) for the years 1976-1982. (A "bomb" is a cyclone that deepens at least one mb per hour for 24 hours.) The works of Colucci (1976) and Sanders and Gyakum (1980) also reveal a good match of the offshore part of component four to the area of maximum deepening of the intense extratropical surface cyclones known as "bombs." Results of Zishka and Smith (1980) show this area to be a preferred area for "non-bomb" cyclones also.

The area of variability over Hudson Bay appears to be related to anticyclone activity. The "bombs" usually develop after the excursion of cold Arctic air out of Canada down the eastern seaboard. This connection will be discussed.

Figure 6b is the spatial phase plot of component four. The phase angles increase to the east and to the southwest from 60°N, 102°W. The portion that moves east corresponds to the area of high variability over Hudson Bay. This area is between 120 to 180 degrees out of phase from the area off the Atlantic Coast. These two coastal centers of variability seem to build in place and die out without much information transferred between them.
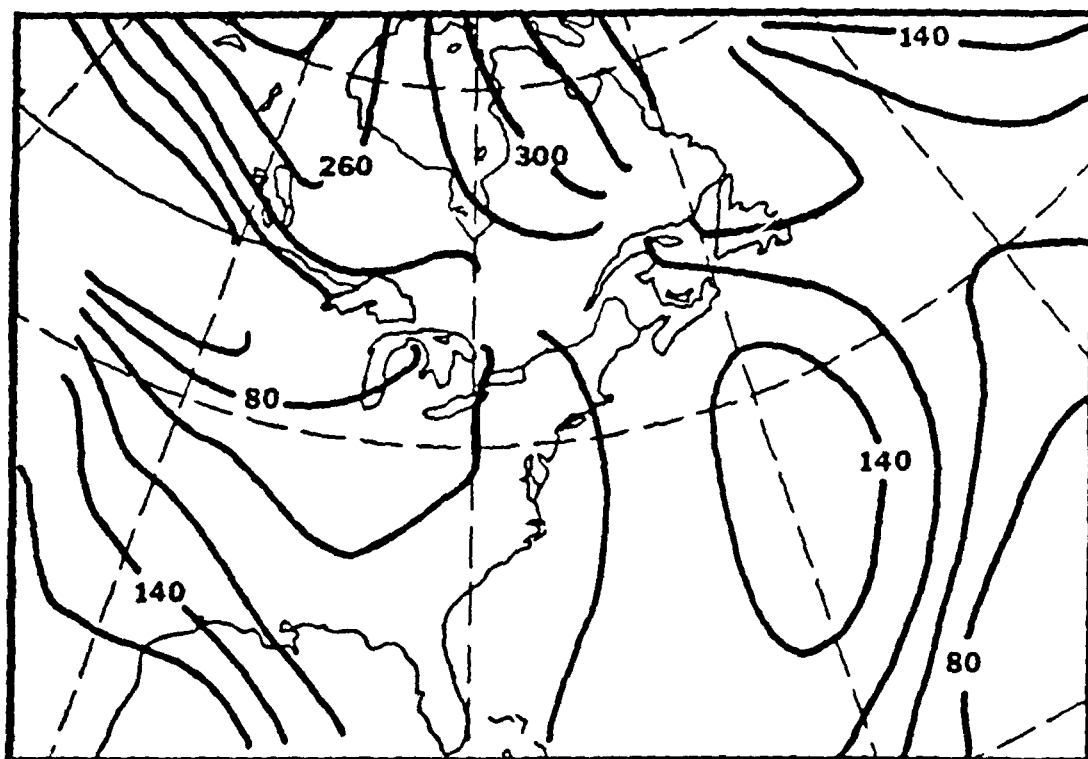
Figure 6b.   The spatial phase (20 degree interval) for component four
of the band-passed filtered data

2) temporal properties

Figure 6c is the temporal amplitude plot of component four. From this plot and table 2 it can be seen that component four was most active in 1974 and the least active in 1981. In 1981 there was a trough at 700 mb over the east coast of North America which forced storms to track further east than normal.

Figure 6d is the temporal phase plot for component four. The plot shows that component four consists of a large number of slow phase changing events and a smaller number of rapid phase changing events.

3) comments

It appears this component picks up the maximum deepening events ("bombs") off the Atlantic Coast and the associated high pressure center of the Arctic air which moves down the eastern seaboard. The question to be asked is why isn't the spatial phase plot showing movement of the anticyclone down the east coast of the US and the movement of the "bombs" up the coast, instead of what appears to be in place development?

The anticyclone area is cut off by a low variability area which resembles the high variability area extension from component two in this area. The shape of this northern area in component four therefore appears to be artificially induced by the CPCA technique.

The coherence check shows (table 1) there is coherence between component one and four. So component one may have already accounted for the overall "average" variability and movement of cyclones off the east coast of the US, while component four captures the most intense deepening and movement stages of these cyclones. As noted by Sanders
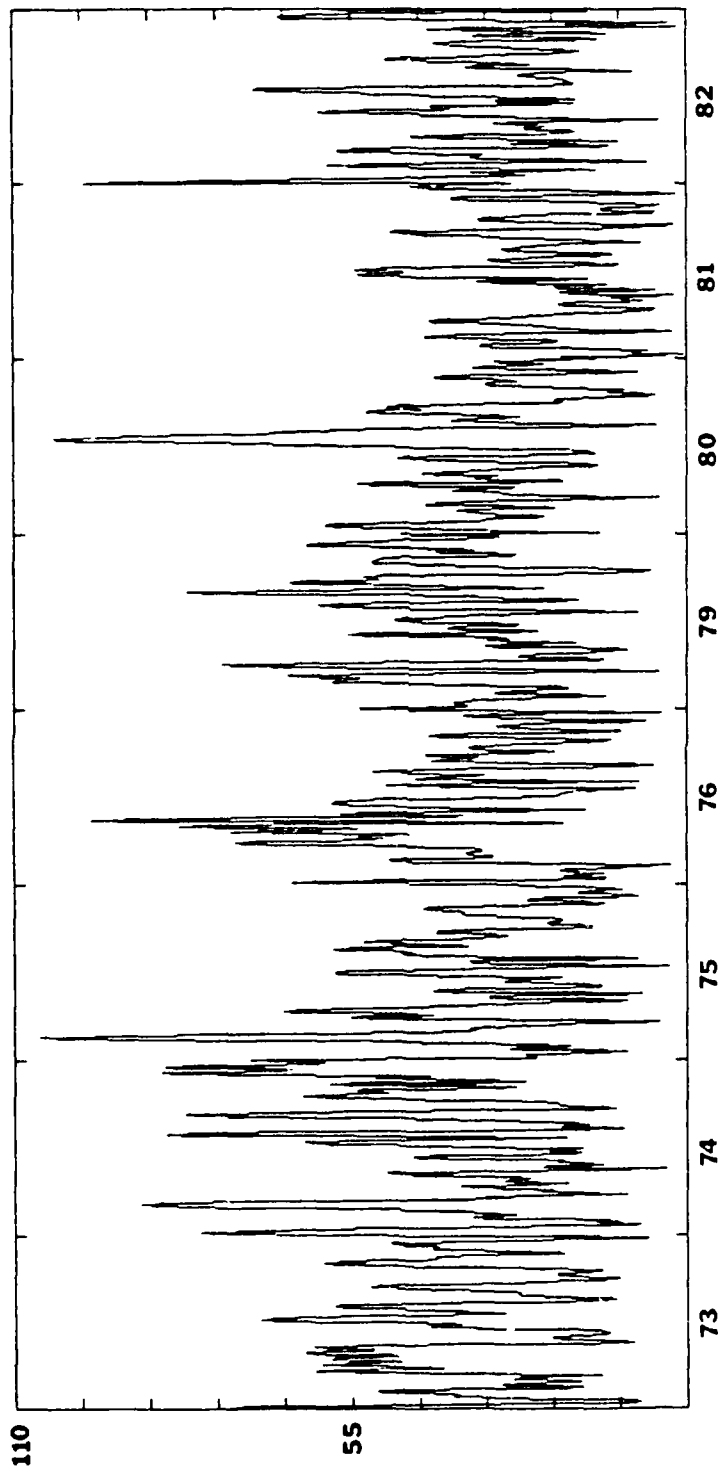
Figure 6c. The temporal amplitude (interval of 11 mb) of component four of the band-passed filtered data, by year
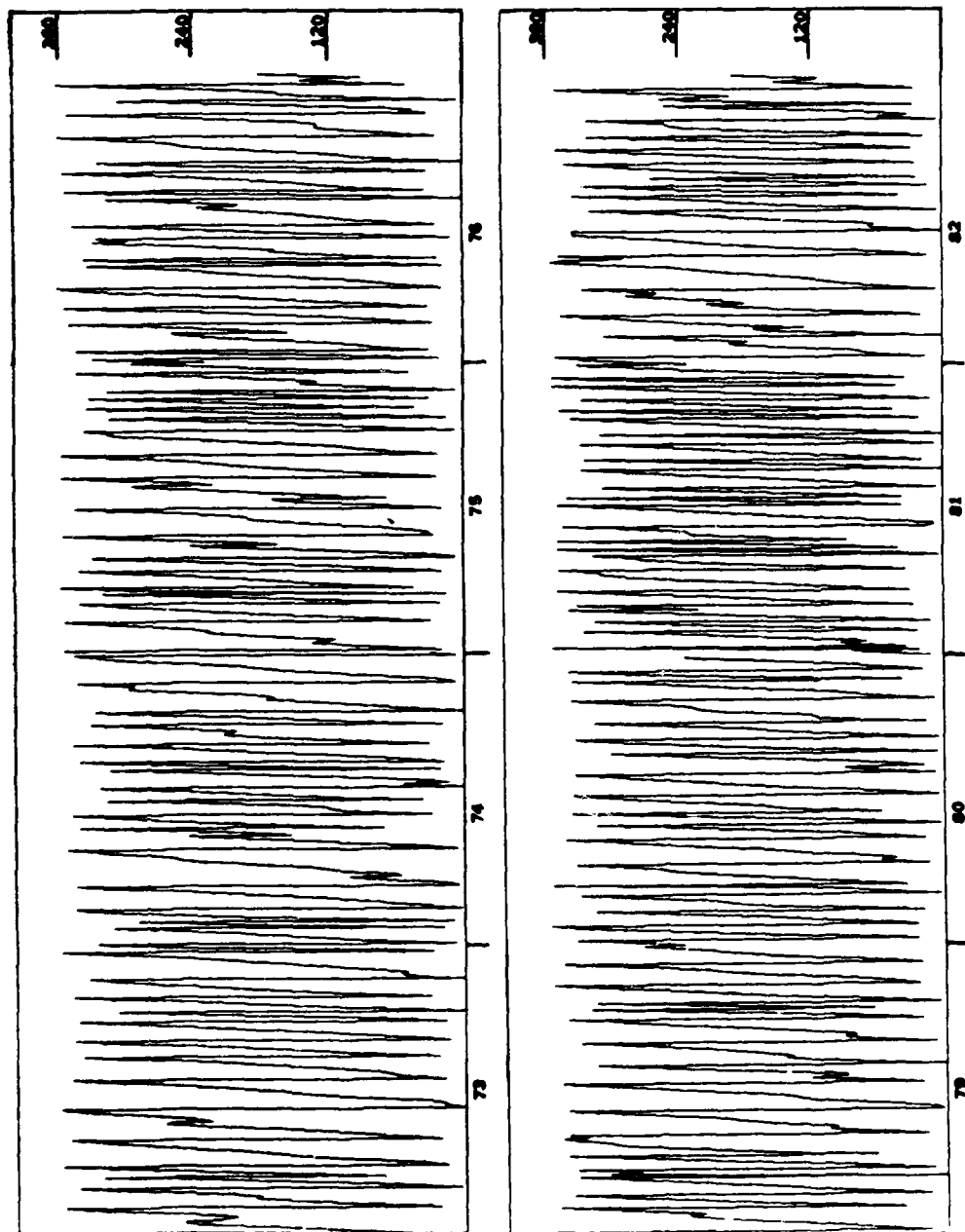
Figure 6d. The temporal phase (degrees) of component four of the band-passed filtered data, by year

and Gyakum (1980), these "bombs" are features of the general
circulation and explode (deepen rapidly) as a result of reaching the
maritime environment off the Atlantic Coast.

6. CONCLUSIONS

A data set was constructed from eight years of wintertime observations (JAN-MAR) of sea level pressure (SLP), and then filtered to eliminate information outside the 2 to 10 day time period. This filter also augmented the original data set with its Hilbert transform. The complex principal component analysis (CPCA) technique was then applied to this augmented data set. This analysis technique is designed to locate regions of spatially large covariability and to detect propagating features in the data field.

The preliminary interpretation of the first four components of the CPCA (accounting for approximately 63.4 percent of the variance in the original data) are as follows:

1) Component one seems to represent the variability pattern that is produced by the movement of anticyclones/cyclones along the mean mid-tropospheric flow. As such, it seems to have some of the other three components mixed in, and they are all correlated as shown by the coherence check (table 1).

2) Component two appears to show two areas of variability. One is along the United States-Canadian border and appears to be caused by anticyclones/cyclones. The other area, just to the east of the Rockies, appears to be linked to the cold air outbreak anticyclones in a north-south direction.

3) Component three seems to show two distinct areas of variability. One is possibly linked to the cold air outbreaks over and to the west of the Rockies. The other area centered over the coast of Labrador is harder to interpret, but appears to be linked to cyclone

activity from the Great Lakes and off the coast of the northeastern United States and eastern Canada.

4) Component four appears to show the outbreak of Arctic air which precedes the possible formation of a rapidly intensifying cyclone called a "bomb" off the Atlantic Coast of North America. This component also appears to show the centers of preferred "bomb" formation areas.

Limitations of the analysis technique appear to have influenced the results obtained. While there are rotation procedures available to overcome these limitations, they appear to have their own limitations and may require the production of a large number of alternate solutions. More work must be done in this area to eliminate the arbitrary phase angle problem.

There is an obvious need for further work in the application of the CPCA technique to a SLP data set, and the subsequent interpretation of the CPCA results as representing synoptic scale disturbances. A few ideas for future research would be to 1) expand the spatial area covered to look at the whole Northern Hemisphere; 2) apply the technique to a larger number of years of data and partition the data into sets by season, and see if the preferred areas shift with the seasonal mean mid-tropospheric flow; 3) apply the technique to a set of data consisting of sea level, 850, 700, 500, and 300 mb pressure, temperature, and height, and see how the analysis of each level and variable fits, or doesn't fit, the general models of the structure of cyclones and anticyclones; and (4) reconstruct an estimate of the original data set from the "significant" components found by the CPCA

technique, and see if the estimated data field displays characteristic pressure patterns and movement expected of synoptic scale disturbances.

As is evident from this study, the interpretation of CPCA results is difficult at times, even with supporting information. Most important, always, is that the results make sense physically and can be found in the original data set.

7. LIST OF REFERENCES

Atmospheric Environment Service, April and June 1973-1979: Weatherwatch. Weatherwise, 26-29, pages vary.

Barber, D. A., J. M. Davis, and A. L. Riordan, 1984: Spectral analysis of station pressure as an indicator of climatological variations in synoptic-scale activity in the eastern United States. Mon. Wea. Rev., 112, 333-339.

Barnett, T. P., 1983: Interaction of the monsoon and Pacific trade wind systems at interannual time scales. Part I: The equatorial zone. Mon. Wea. Rev., 111, 756-773.

Blackmon, M. L., 1976: A climatological spectral study of the 500 mb geopotential height of the Northern Hemisphere. J. Atmos. Sci., 33, 1607-1623.

_____, and G. H. White, 1982: Zonal wavenumber characteristics of Northern Hemisphere transient eddies. J. Atmos. Sci., 39, 1985-1998.

_____, J. M. Wallace, N.-C. Lau, and S. L. Mullen, 1977: An observational study of the Northern Hemisphere wintertime circulation. J. Atmos. Sci.., 34, 1040-1053.

_____, R. A. Madden, J. M. Wallace, and D. S. Gutzler, 1979: Geographical variations in the vertical structure of geopotential height fluctuations. J. Atmos. Sci., 36, 2450-2466.

_____, Y.-H. Lee, and J. M. Wallace, 1984a: Horizontal structure of 500 mb height fluctuations with long, intermediate, and short time scales. J. Atmos. Sci., 41, 961-979.

_____, Y.-H. Lee, J. M. Wallace, and H.-H. Hsu, 1984b: Time variation of 500 mb height fluctuations with long, intermediate, and short-time scales as decuded from lag-correlation statistics. J. Atmos. Sci., 41, 981-991.

Bowie, E. H., and R. H. Weightman, 1914: Types of storms of the United States and their average movement. Mon. Wea. Rev., Sup. 1, 37 pp., 114 charts.

Cizek, V., 1970: Discrete Hilbert transform. IEEE Trans. Aud. Elect., AU-18, 340-343.

Climatological Data, National Summary, January, February, and March 1973-1976 and 1979-1980. NOAA/EDIS, National Climatic Center, Asheville.

Colucci, S. J., 1976: Winter cyclone frequencies over the eastern United States and adjacent western Atlantic, 1964-1973. Bull. Amer. Meteor. Soc., 57, 548-553.

Green, P. E., 1978: Analyzing Multivariate Data. Dryden Press, pp. 341-390.

Hartmann, D. L., 1974: Time spectral analysis of mid-latitude disturbance. Mon. Wea. Rev., 102, 348-362.

Hayden, B. P., and W. Smith, 1982: Season-to-season cyclone frequency prediction. Mon. Wea. Rev., 110, 239-253.

Holl, M. M., and B. R. Mendenhall, 1971: The FIB Methodology and Application Meteorology International, California. Project M-167 Final Report, Fleet Numerical Weather Center, Contract No. N66314-70-C-5226. 65 pp.

Horel, J. D., 1981: A rotated principal component analysis of the interannual variability of the Northern Hemisphere 500 mb height field. Mon. Wea. Rev., 109, 2080-2092.

_____, 1984: Complex principal component analysis: Theory and examples. J. Climate Appl. Meteor., 23, 1660-1673.

Jeene, R. L., 1970: The NMC octagonal grid. NCAR unnumbered writeup. [Available from Roy L. Jenne, NCAR, P.O. Box 3000, Boulder, CO., 80307]

_____, 1975: Data sets for meteorological research. NCAR Tech. Note TN/1A-111.

Johnston, R. J., 1978: Multivariate Statistical Analysis in Geography. Chaucer Press, pp. 127-182.

Klein, W., 1951a: A hemispheric study of daily pressure variability at sea level and aloft. J. Meteor., 8, 332-346.

_____, 1951b: The weather and circulation of December 1951. Mon. Wea. Rev., 79, 218-221.

_____, 1957: Principal tracks and mean frequencies of cyclones and anticyclones in the Northern Hemisphere. Res. Paper No. 40, U.S. Weather Bureau, Washington, D.C., 60 pp.

_____, 1958: The frequency of cyclones and anticyclones in relation to the mean circulation. J. of Meteor., 15, 98-102.

_____, 1967: Specification of sea-level pressure from 700-mb height. Quart. J. Roy. Meteor. Soc., 93, 214-226.

Kutzbach, J. E., 1967: Empirical eigenvectors of sea-level pressure, surface temperature and precipitation complexes over North America. J. Appl. Meteor., 6, 791-802.

_____, 1970: Large-scale features of monthly mean Northern Hemisphere anomaly maps of sea-level pressure. Mon. Wea. Rev., 98, 708-716.

Ludlum, D. M., April and June 1979-1982: Weatherwatch. Weatherwise, 32-35, pages vary.

Michaelsen, J., 1982: A statistical study of large-scale, long-period variability in North Pacific sea surface temperature anomalies. J. of Phy. Oceanogr., 12, 694-703.

Miller, E. C., 1932: Relative frequency of centers of cyclones and anticyclones in the United States. Mon. Wea. Rev., 60, 6-11.

North, G. R., T. L. Bell, R. F. Cahalan, and F. J. Moneg, 1982: Sampling errors in the estimation of empirical orthogonal functions. Mon. Wea. Rev., 110, 699-706.

Palmen, E., and C. W. Newton, 1969: Atmospheric Circulation Systems. Academic Press, pp. 92-97.

Petterssen, S., 1956: Weather Analysis and Forecasting, Vol. I, 2nd ed. McGraw-Hill, pp. 232-281.

Rasmusson, E. M., P. A. Arkin, W. Y. Chen, and J. B. Jalickee, 1981: Biennial variations in surface temperature over the United States as revealed by singular decomposition. Mon. Wea. Rev., 109, 587-598.

Reitan, C. H., 1974: Frequencies of cyclones and cyclogenesis for North America. Mon. Wea. Rev., 102, 861-868.

Richman, M. B., 1981: Obliquely rotated principal components: An improved meteorological map typing technique. J. Climate Appl. Meteor., 20, 1145-1159.

Roebber, P. J., 1984: Statistical analysis and updated climatology of explosive cyclones. Mon. Wea. Rev., 112, 1577-1589.

Sanders, F., and J. R. Gyakum, 1980: Synoptic-dynamic climatology of the "Bomb." Mon. Wea. Rev., 108, 1589-1606.

Wallace, J. M., and R. E. Dickinson, 1972: Empirical orthogonal representation of time series in the frequency domain. Part I: Theoretical considerations. J. Appl. Meteor., 11, 887-892.

Wasko, P. E., 1954: Pressure and temperature variation over the centers of typical migratory anticyclones. <u>Bull. Amer. Meteor. Soc.</u>, 35, 26-32.

Weather Bureau, 1952: Normal weather charts for the Northern Hemisphere. Tech. Paper No. 21, U.S. Weather Bureau, Washington, D.C., 74 pp.

White, G. H., 1980: On the observed spatial scales of Northern Hemisphere transient motions. <u>J. Atmos. Sci.</u>, 37, 892-894.

Whittaker, L. M., and L. H. Horn, 1981: Geographical and seasonal distribution of North American cyclogenesis, 1958-1977. <u>Mon. Wea. Rev.</u>, 109, 2312-2322.

Zishka, K. M., and P. J. Smith, 1980: The climatology of cyclones and anticyclones over North America and surrounding ocean environs for January and July, 1950-77. <u>Mon. Wea. Rev.</u>, 108, 387-401.

ABSTRACT

ESTIS, FRANK L. Complex Principal Component Analysis of Sea Level
Pressure over Eastern North America and the Western Atlantic Ocean: A
Search for Preferred Disturbance Activity Areas. (Under the direction
of JERRY M. DAVIS.)

The purpose of this study was to identify preferred areas of
synoptic scale disturbance activity through the use of the objective
analysis technique called complex principal component analysis. The
analysis technique was applied to a sea level pressure data set
consisting of twice daily observations (00 and 12 GMT) during the
months of January, February, and March, for the years 1973-1976 and
1979-1982. The months of January through March were chosen to
encompass the time frame of the Genesis of Atlantic Lows Experiment
1986. This experiment was designed to study the evolution of cyclones
along the Atlantic Coast of the United States, because these cyclones
can become quite intense during the winter months and pose a threat to
ocean shipping activities and coastal regions of the United States and
Canada. The geographical area studied extended approximately from
$30^{o}-120^{o}W$ and from $25^{o}-60^{o}N$, on a polar stereographic map projection.

The complex principal component analysis technique allows the
detection of propagating features in the pressure data set. The
original data set is augmented with its own Hilbert transform, which is
nearly equivalent in the time domain to the quadrature spectrum in the
frequency domain. This augmented data set thus contains information on
the relative phase relationships among the propagating features of the
data set.

The eigenvalues, complex eigenvectors (components), and complex component scores are extracted from the augmented data matrix and used to compute four measures that define possible propagating features of the data set. When the component's values are plotted, at their respective grid points, the patterns can be seen that account for the largest amount of variance (first component), the second largest amount of variance (second component), and so on, in the sea level pressure data.

The variance in the pressure field is felt to be a direct reflection of disturbance activity. Furthermore, when the data are filtered to a "synoptic scale" frequency window, the variance in the pressure field corresponds closely with cyclone and anticyclone storm tracks over a time period of 2-10 days. This spatial and temporal correspondence between synoptic scale disturbances and variance of pressure allows the use of the complex principal component analysis technique on the filtered sea level pressure data set to objectively find preferred areas of disturbance activity.

The results of the analysis produced four components that could be given a preliminary interpretation from a physical sense. The components (patterns) resembled areas of activity as discovered in previous studies using other analysis techniques. Component one resembled the variability pattern produced by the movement of anticyclones/cyclones guided by the mean mid-tropospheric flow. Component two represented the cold air outbreak anticyclones to the east of the Rockies, and anticyclones/cyclones which move along the United States-Canadian border. Component three is linked to the cold

air outbreak anticyclones to the west of the Rockies, and to cyclone activity over the Great Lakes and off the coast of the northeastern United States and eastern Canada. Component four represents the formation of the "bomb" cyclone off the Atlantic Coast of North Carolina, and the preceding Arctic air outbreak anticyclone. The results are not without ambiguities, and these are discussed also.

END
10-86
DTIC